

University of Windsor

## Scholarship at UWindor

---

Electronic Theses and Dissertations

Theses, Dissertations, and Major Papers

---

1994

### Constructing Voronoi diagrams in $L(1)$ and $L(\infty)$ metrics with two plane sweeps.

Jianan. Wang  
*University of Windsor*

Follow this and additional works at: <https://scholar.uwindsor.ca/etd>

---

#### Recommended Citation

Wang, Jianan., "Constructing Voronoi diagrams in  $L(1)$  and  $L(\infty)$  metrics with two plane sweeps." (1994). *Electronic Theses and Dissertations*. 1555.  
<https://scholar.uwindsor.ca/etd/1555>

This online database contains the full-text of PhD dissertations and Masters' theses of University of Windsor students from 1954 forward. These documents are made available for personal study and research purposes only, in accordance with the Canadian Copyright Act and the Creative Commons license—CC BY-NC-ND (Attribution, Non-Commercial, No Derivative Works). Under this license, works must always be attributed to the copyright holder (original author), cannot be used for any commercial purposes, and may not be altered. Any other use would require the permission of the copyright holder. Students may inquire about withdrawing their dissertation and/or thesis from this database. For additional inquiries, please contact the repository administrator via email ([scholarship@uwindsor.ca](mailto:scholarship@uwindsor.ca)) or by telephone at 519-253-3000ext. 3208.



National Library  
of Canada

Acquisitions and  
Bibliographic Services Branch

395 Wellington Street  
Ottawa, Ontario  
K1A 0N4

Bibliothèque nationale  
du Canada

Direction des acquisitions et  
des services bibliographiques

395, rue Wellington  
Ottawa (Ontario)  
K1A 0N4

*Your file* *Votre référence*

*Our file* *Notre référence*

## NOTICE

The quality of this microform is heavily dependent upon the quality of the original thesis submitted for microfilming. Every effort has been made to ensure the highest quality of reproduction possible.

If pages are missing, contact the university which granted the degree.

Some pages may have indistinct print especially if the original pages were typed with a poor typewriter ribbon or if the university sent us an inferior photocopy.

Reproduction in full or in part of this microform is governed by the Canadian Copyright Act, R.S.C. 1970, c. C-30, and subsequent amendments.

## AVIS

La qualité de cette microforme dépend grandement de la qualité de la thèse soumise au microfilmage. Nous avons tout fait pour assurer une qualité supérieure de reproduction.

S'il manque des pages, veuillez communiquer avec l'université qui a conféré le grade.

La qualité d'impression de certaines pages peut laisser à désirer, surtout si les pages originales ont été dactylographiées à l'aide d'un ruban usé ou si l'université nous a fait parvenir une photocopie de qualité inférieure.

La reproduction, même partielle, de cette microforme est soumise à la Loi canadienne sur le droit d'auteur, SRC 1970, c. C-30, et ses amendements subséquents.

Canada

**Constructing Voronoi Diagrams in  $L_1$   
and  $L_\infty$  Metrics with Two Plane Sweeps**

**by**

**Jianan Wang**

**A Thesis**

**Submitted to the Faculty of Graduate Studies and Research  
through the School of Computer Science in Partial  
Fulfillment of the Requirements for the Degree of  
Master of Science at the  
University of Windsor  
Windsor, Ontario, Canada  
1994**



National Library  
of Canada

Acquisitions and  
Bibliographic Services Branch

395 Wellington Street  
Ottawa, Ontario  
K1A 0N4

Bibliothèque nationale  
du Canada

Direction des acquisitions et  
des services bibliographiques

395, rue Wellington  
Ottawa (Ontario)  
K1A 0N4

*Your file    Votre référence*

*Our file    Notre référence*

THE AUTHOR HAS GRANTED AN  
IRREVOCABLE NON-EXCLUSIVE  
LICENCE ALLOWING THE NATIONAL  
LIBRARY OF CANADA TO  
REPRODUCE, LOAN, DISTRIBUTE OR  
SELL COPIES OF HIS/HER THESIS BY  
ANY MEANS AND IN ANY FORM OR  
FORMAT, MAKING THIS THESIS  
AVAILABLE TO INTERESTED  
PERSONS.

L'AUTEUR A ACCORDE UNE LICENCE  
IRREVOCABLE ET NON EXCLUSIVE  
PERMETTANT A LA BIBLIOTHEQUE  
NATIONALE DU CANADA DE  
REPRODUIRE, PRETER, DISTRIBUER  
OU VENDRE DES COPIES DE SA  
THESE DE QUELQUE MANIERE ET  
SOUS QUELQUE FORME QUE CE SOIT  
POUR METTRE DES EXEMPLAIRES DE  
CETTE THESE A LA DISPOSITION DES  
PERSONNE INTERESSEES.

THE AUTHOR RETAINS OWNERSHIP  
OF THE COPYRIGHT IN HIS/HER  
THESIS. NEITHER THE THESIS NOR  
SUBSTANTIAL EXTRACTS FROM IT  
MAY BE PRINTED OR OTHERWISE  
REPRODUCED WITHOUT HIS/HER  
PERMISSION.

L'AUTEUR CONSERVE LA PROPRIETE  
DU DROIT D'AUTEUR QUI PROTEGE  
SA THESE. NI LA THESE NI DES  
EXTRAITS SUBSTANTIELS DE CELLE-  
CI NE DOIVENT ETRE IMPRIMES OU  
AUTREMENT REPRODUITS SANS SON  
AUTORISATION.

ISBN 0-612-01426-6

Canada

Name

Tianan Wang

Dissertation Abstracts International is arranged by broad, general subject categories. Please select the one subject which most nearly describes the content of your dissertation. Enter the corresponding four-digit code in the spaces provided.

Computer Science

SUBJECT TERM

0989

U·M·I

SUBJECT CODE

## Subject Categories

## THE HUMANITIES AND SOCIAL SCIENCES

## COMMUNICATIONS AND THE ARTS

Architecture ..... 0729  
Art History ..... 0377  
Cinema ..... 0900  
Dance ..... 0378  
Fine Arts ..... 0357  
Information Science ..... 0723  
Journalism ..... 0391  
Library Science ..... 0399  
Mass Communications ..... 0708  
Music ..... 0413  
Speech Communication ..... 0459  
Theater ..... 0465

## EDUCATION

General ..... 0515  
Administration ..... 0514  
Adult and Continuing ..... 0516  
Agricultural ..... 0517  
Art ..... 0273  
Bilingual and Multicultural ..... 0282  
Business ..... 0688  
Community College ..... 0275  
Curriculum and Instruction ..... 0727  
Early Childhood ..... 0518  
Elementary ..... 0524  
Finance ..... 0277  
Guidance and Counseling ..... 0519  
Health ..... 0680  
Higher ..... 0745  
History of ..... 0520  
Home Economics ..... 0278  
Industrial ..... 0521  
Language and Literature ..... 0279  
Mathematics ..... 0280  
Music ..... 0522  
Philosophy of ..... 0998  
Physical ..... 0523

Psychology ..... 0525  
Reading ..... 0535  
Religious ..... 0527  
Sciences ..... 0714  
Secondary ..... 0533  
Social Sciences ..... 0534  
Sociology of ..... 0340  
Special ..... 0529  
Teacher Training ..... 0530  
Technology ..... 0710  
Tests and Measurements ..... 0288  
Vocational ..... 0747

## LANGUAGE, LITERATURE AND LINGUISTICS

Language ..... 0679  
General ..... 0289  
Ancient ..... 0290  
Linguistics ..... 0291  
Modern ..... 0401  
Literature ..... 0294  
General ..... 0295  
Classical ..... 0297  
Comparative ..... 0298  
Medieval ..... 0316  
Modern ..... 0591  
African ..... 0305  
American ..... 0352  
Asian ..... 0355  
Canadian (English) ..... 0593  
Canadian (French) ..... 0311  
English ..... 0312  
Germanic ..... 0315  
Latin American ..... 0313  
Middle Eastern ..... 0314  
Romance ..... 0314  
Slavic and East European

## PHILOSOPHY, RELIGION AND THEOLOGY

Philosophy ..... 0422  
Religion ..... 0318  
General ..... 0321  
Biblical Studies ..... 0319  
Clergy ..... 0320  
History of ..... 0322  
Philosophy of ..... 0469  
Theology

## SOCIAL SCIENCES

American Studies ..... 0323  
Anthropology ..... 0324  
Archaeology ..... 0326  
Cultural ..... 0327  
Physical ..... 0310  
Business Administration ..... 0272  
General ..... 0770  
Accounting ..... 0454  
Banking ..... 0338  
Management ..... 0385  
Marketing ..... 0501  
Canadian Studies ..... 0503  
Economics ..... 0505  
General ..... 0508  
Agricultural ..... 0509  
Commerce-Business ..... 0510  
Finance ..... 0511  
History ..... 0358  
Labor ..... 0366  
Theory ..... 0351  
Folklore ..... 0578  
Geography ..... 0578  
Gerontology ..... 0578  
History

Ancient ..... 0579  
Medieval ..... 0581  
Modern ..... 0582  
Black ..... 0328  
African ..... 0331  
Asia, Australia and Oceania ..... 0332  
Canadian ..... 0334  
European ..... 0335  
Latin American ..... 0336  
Middle Eastern ..... 0333  
United States ..... 0337  
History of Science ..... 0585  
Law ..... 0398  
Political Science ..... 0615  
General ..... 0616  
International Law and Relations ..... 0617  
Public Administration ..... 0814  
Recreation ..... 0452  
Social Work ..... 0626  
Sociology ..... 0627  
General ..... 0928  
Criminology and Penology ..... 0631  
Demography ..... 0628  
Ethnic and Racial Studies ..... 0629  
Individual and Family ..... 0630  
Studies ..... 0700  
Industrial and Labor ..... 0344  
Relations ..... 0709  
Public and Social Welfare ..... 0999  
Social Structure and Development ..... 0453  
Theory and Methods ..... 0453  
Transportation ..... 0453  
Urban and Regional Planning ..... 0453  
Women's Studies

## THE SCIENCES AND ENGINEERING

## BIOLOGICAL SCIENCES

Agriculture ..... 0473  
General ..... 0285  
Agronomy ..... 0475  
Animal Culture and Nutrition ..... 0476  
Animal Pathology ..... 0359  
Food Science and Technology ..... 0478  
Forestry and Wildlife ..... 0479  
Plant Culture ..... 0480  
Plant Pathology ..... 0817  
Plant Physiology ..... 0777  
Range Management ..... 0746  
Wood Technology ..... 0306  
Biology ..... 0287  
General ..... 0308  
Anatomy ..... 0309  
Biostatistics ..... 0379  
Botany ..... 0329  
Cell ..... 0353  
Ecology ..... 0369  
Entomology ..... 0793  
Genetics ..... 0410  
Limnology ..... 0307  
Microbiology ..... 0317  
Molecular ..... 0416  
Neuroscience ..... 0433  
Oceanography ..... 0821  
Physiology ..... 0778  
Radiation ..... 0472  
Veterinary Science ..... 0786  
Zoology ..... 0760  
Biophysics ..... 0425  
General ..... 0996  
Medical

## EARTH SCIENCES

Biogeochemistry ..... 0425  
Geochemistry ..... 0996

Geodesy ..... 0370  
Geology ..... 0372  
Geophysics ..... 0373  
Hydrology ..... 0388  
Mineralogy ..... 0411  
Paleobotany ..... 0345  
Paleoecology ..... 0426  
Paleontology ..... 0418  
Paleozoology ..... 0985  
Palynology ..... 0427  
Physical Geography ..... 0368  
Physical Oceanography ..... 0415

## HEALTH AND ENVIRONMENTAL SCIENCES

Environmental Sciences ..... 0768  
Health Sciences ..... 0566  
General ..... 0300  
Audiology ..... 0992  
Chemotherapy ..... 0567  
Dentistry ..... 0350  
Education ..... 0769  
Hospital Management ..... 0758  
Human Development ..... 0982  
Immunology ..... 0564  
Medicine and Surgery ..... 0347  
Mental Health ..... 0569  
Nursing ..... 0570  
Nutrition ..... 0380  
Obstetrics and Gynecology ..... 0354  
Occupational Health and Therapy ..... 0381  
Ophthalmology ..... 0571  
Pathology ..... 0419  
Pharmacology ..... 0572  
Pharmacy ..... 0382  
Physical Therapy ..... 0573  
Public Health ..... 0574  
Radiology ..... 0575  
Recreation

Speech Pathology ..... 0460  
Toxicology ..... 0383  
Home Economics ..... 0386

## PHYSICAL SCIENCES

Pure Sciences ..... 0485  
Chemistry ..... 0749  
General ..... 0486  
Agricultural ..... 0487  
Analytical ..... 0488  
Biochemistry ..... 0738  
Inorganic ..... 0490  
Nuclear ..... 0491  
Organic ..... 0494  
Pharmaceutical ..... 0495  
Physical ..... 0754  
Polymer ..... 0405  
Radiation ..... 0605  
Mathematics ..... 0986  
Physics ..... 0606  
General ..... 0608  
Acoustics ..... 0748  
Astronomy and Astrophysics ..... 0607  
Atmospheric Science ..... 0607  
Atomic ..... 0607  
Electronics and Electricity ..... 0798  
Elementary Particles and High Energy ..... 0759  
Fluid and Plasma ..... 0609  
Molecular ..... 0610  
Nuclear ..... 0752  
Optics ..... 0756  
Radiation ..... 0611  
Solid State ..... 0463  
Statistics ..... 0346  
Applied Sciences ..... 0984  
Applied Mechanics ..... 0984  
Computer Science

Engineering ..... 0537  
General ..... 0538  
Aerospace ..... 0539  
Agricultural ..... 0540  
Automotive ..... 0541  
Biomedical ..... 0542  
Chemical ..... 0543  
Civil ..... 0544  
Electronics and Electrical ..... 0348  
Heat and Thermodynamics ..... 0545  
Hydraulic ..... 0546  
Industrial ..... 0547  
Marine ..... 0794  
Materials Science ..... 0548  
Mechanical ..... 0743  
Metallurgy ..... 0551  
Mining ..... 0552  
Nuclear ..... 0549  
Packaging ..... 0765  
Petroleum ..... 0554  
Sanitary and Municipal ..... 0790  
System Science ..... 0428  
Geotechnology ..... 0796  
Operations Research ..... 0795  
Plastics Technology ..... 0994  
Textile Technology

## PSYCHOLOGY

General ..... 0621  
Behavioral ..... 0384  
Clinical ..... 0622  
Developmental ..... 0620  
Experimental ..... 0623  
Industrial ..... 0624  
Personality ..... 0625  
Physiological ..... 0989  
Psychobiology ..... 0349  
Psychometrics ..... 0632  
Social ..... 0451



**Jianan Wang 1994**  
**© All Rights Reserved**

## Abstract

A plane-sweep method without using transformation but using two sweeps is used to construct the Voronoi diagram in  $L_1$  ( $L_\infty$ , respectively) metric of a set of  $n$  point sites in  $O(n \log n)$  time and  $O(n)$  space. The two sweeps advance from opposite directions and produce two symmetrical data structures called the Left-to-Right Shortest-Path-Map and Right-to-Left Shortest-Path-Map. The two maps are then tailored to produce the desired Voronoi diagram.

*To my wife Qiu and son Zhen*



## **Acknowledgments**

I would like to take this opportunity to give the deepest thanks to my supervisor Dr. Y.H.Tsin for his constant guidance, encouragement, understanding, and financial support.

I extend my gratitude to my thesis internal examiner Dr. H.Towes and external examiner Dr. H.K.Kwan for providing valuable comments.

My thanks go as well to Dr. R.Frost, Dr. S.Bandyopadhyay, Dr. J.Morrissey, Dr. R.Kent, Dr. L.Li, and Dr. Y.Park for their good advice and inspiration.

I would also like to thank Steve Karamatos, Walid Nyamneh and our secretaries Mary and Josette for their help.

Finally, I cannot miss this opportunity to express my thanks to all my graduate lab fellows who sit down with me day and night in front of the computers.

# TABLE OF CONTENTS

Abstract . . . . .	iv
Acknowledgments . . . . .	vi
List of Figures . . . . .	x
1 An Overview of Voronoi diagrams . . . . .	1
1.1 An Overview . . . . .	1
1.1.1 The Original Voronoi Diagram Problem . . . . .	1
1.1.2 Voronoi Diagram in $L_p$ Metric . . . . .	2
1.1.3 Voronoi Diagrams and Convex Hulls . . . . .	3
1.1.4 Other Generalizations of Voronoi Diagram . . . . .	3
1.1.4.1 The Voronoi Diagram of a Set of Objects other than Points . . . . .	3
1.1.4.2 Higher-order Voronoi Diagrams (in a Plane) . . . . .	4
1.1.4.3 Weighted Voronoi Diagrams . . . . .	5
1.1.4.4 Voronoi Diagram in High Dimensions . . . . .	5
1.1.4.5 Voronoi Diagrams Involving Obstacles . . . . .	6
1.2 Techniques for Constructing the Voronoi Diagram . . . . .	6
1.2.1 The Incremental approach . . . . .	6
1.2.2 Divide-conquer approach . . . . .	7

1.2.3	Sweep line approach . . . . .	10
1.2.4	Two plane sweep approach . . . . .	12
1.2.5	A comparison of three methods . . . . .	13
2	Voronoi Diagrams in $L_1$ and $L_\infty$ Metrics . . . . .	14
2.1	Voronoi Diagrams in $L_1$ and $L_\infty$ Metrics . . . . .	14
2.1.1	$L_1$ Metric . . . . .	14
2.1.2	$L_\infty$ metric . . . . .	17
2.1.3	The Isometry of $L_1$ and $L_\infty$ . . . . .	17
2.1.4	The applications of $L_1$ and $L_\infty$ metrics in two-dimensional storage. . . . .	19
2.2	Construction the Voronoi diagram in $L_1$ and $L_\infty$ metrics by Divide and Conquer . . . . .	20
3	Using Two Sweeps to Construct the Voronoi Diagrams in $L_1$ Metric . . . . .	24
3.1	Shortest-Path-Map . . . . .	24
3.2	The Construction of Shortest-Path-Map (SPM) . . . . .	27
3.2.1	The Construction of $SPM_{\vdash}(S)$ ( $SPM_{\dashv}(S)$ ) . . . . .	31
3.3	Constructing the Voronoi Diagram from two Shortest-Path-Maps . . . . .	41
3.3.1	Finding the type 1 Voronoi arcs . . . . .	42

3.3.2	Finding the type 2 Voronoi arcs . . . . .	46
3.3.3	A special case discussion: . . . . .	46
3.4	Algorithms . . . . .	49
4	Conclusions . . . . .	64
APPENDIX	An Algorithm for Constructing the Left to Right Shortest Path Map ( $SPM_{\vdash}(S)$ ) . . . . .	65
APPENDIX	An Algorithm for Constructing the Voronoi Diagram in $L_1$ Metric . . . . .	68
APPENDIX	An Example of Constructing the Voronoi Diagram in $L_1$ Metric . . . . .	72
BIBLIOGRAPHY	. . . . .	81

## List of Figures

Figure 1	A set of sites in a plane is divided into two approximately equal parts . . . . .	8
Figure 2	The Voronoi diagram of the left subset $Vor(S_L)$ and the Voronoi diagram of the right subset $Vor(S_R)$ are merged into one . . . . .	9
Figure 3	A geometric transformation to Voronoi diagram . .	12
Figure 4	Different types of bisectors of $q_i$ and $q_j$ that divide the plane into region $R(q_i)$ and $R(q_j)$ . . . . .	15
Figure 5	Voronoi diagram in $L_1$ metric. . . . .	17
Figure 6	The isometry of $L_1$ and $L_\infty$ metrics . . . . .	19
Figure 7	Merging left subset and right subset. . . . .	21
Figure 8	Tracing $T$ in $V(L_1)$ without backtracking. . . . .	23
Figure 9	A left-to-right shortest-path-map and a right-to-left shortest-path-map . . . . .	26
Figure 10	$d_1(s_i, w) < d_1(s_h, w)$ . . . . .	28
Figure 11	The upper boundary and lower boundary of an initial region $\Delta(s_i)$ . . . . .	29
Figure 12	The beginning of the $SPM_{\leftarrow}(S)$ . . . . .	32

Figure 13	The corresponding DCEL represents part of the $SPM_{l-}(S)$ . . . . .	32
Figure 14	$SPM_{l-}(S)$ when sweep line $l_3$ passes through $s_3$	34
Figure 15	The corresponding DCEL represents the $SPM_{l-}(S)$ . when sweep line passes through $s_3$ .	34
Figure 16	Using the balanced binary search tree to find the initial region $\Delta(s_i)$ in $O(\log n)$ time. . . . .	37
Figure 17	The balanced binary search tree $T$ is an empty tree. . . . .	38
Figure 18	The edges enclosing one field are grouped together. . . . .	39
Figure 19	Type 1 and type 2 Voronoi arcs . . . . .	42
Figure 20	Point $u$ is the centre of sites $s_i$ , $s_j$ , and $s_k$ . . . . .	44
Figure 21	Type 1 Voronoi arcs . . . . .	45
Figure 22	Three type 2 Voronoi arcs meet at one point . . .	47
Figure 23	Type 2 Voronoi arcs . . . . .	48
Figure 24	Type 2 Voronoi arc tree. . . . .	49
Figure 25	Areas $\Delta(s_1) \cap \Delta_{opp}(s_3)$ represented by $\{1, 3\}$ have no type 2 Voronoi arcs inside. . . . .	51

Figure 26	Start tracing back the type 2 Voronoi arc tree from (a) a h_SPM arc with the ending point at infinity, or from (b) a type 1 Voronoi arc. . . . .	54
Figure 27	Tracing back from a type 2 Voronoi arc to another type 2 Voronoi arc, and meet a type 1 Voronoi arc as a root of a new type 2 Voronoi arc tree. . . . .	55
Figure 28	Tracing back from a type 2 Voronoi arc to (a) a h_SPM arc with the ending point at infinity. (b) a type 1 Voronoi arc which is met by other type 2 Voronoi arc tree. . . . .	56
Figure 29	Three type 2 Voronoi arcs meet together. . . . .	59
Figure 30	Three type 2 Voronoi arcs meet together. Tracing type 2 Voronoi arc trees from edge $\overline{ap}$ . . . . .	61

## **Chapter 1 An Overview of Voronoi diagrams**

### **Section 1 An Overview**

The Voronoi diagram for a set of  $n$  points in the Euclidean plane is a classic geometric object named after the Russian mathematician G.Voronoi [32, 33]. It was introduced to the field of computer science in 1975 by Shamos and Hoey [27]. As the Voronoi diagram has many useful applications in various areas of science (eg. pattern recognition, robotics, etc), it has drawn considerable research interest over the last two decades. Many varieties of Voronoi diagrams have been proposed and many efficient algorithms have been designed to construct them.

#### **The Original Voronoi Diagram Problem**

**Definition:** Let  $S$  be a finite set of points on the plane  $R^2$ . For each site  $s \in S$ , the Voronoi region of  $s$  is the set:

$$V(s) = \{p \in R^2 | d(p, s) \leq d(p, t), \text{ for every } t \in S\}$$

where  $d$  is the Euclidean distance function. The Voronoi diagram of  $S$  is the set:

$$Vor(S) = \{V(s) | s \in S\}$$

Clearly, the Voronoi diagram for a set of points on the plane is a partition of the plane into  $n$  polygon regions, each of which is associated with a given point.



The region associated with a point is the locus of points closer to that point than to any other given point in  $S$ .

Shamos and Hoey [27] used the divide-conquer method to create the  $Vor(S)$ . Fortune [8] used a plane sweep method with transformation to construct the same diagram. Both achieved the  $O(n \log n)$  time and  $O(n)$  space bound which have been shown to be optimal [29].

Once the Voronoi diagram is available, many important proximity problems such as the all-nearest-neighbor problem, the triangulation problem, and the EMST (Euclidean Minimum Spanning Tree) problem can be solved in  $O(n)$  time.

### **Voronoi Diagram in $L_p$ Metric**

The Voronoi diagram discussed above is referred to as the Euclidean metric, which is called  $L_2$  metric in Minkowski's formulation. The diagram can be naturally extended to the  $L_p$  metric where  $1 \leq p \leq \infty$ . The definition of  $L_p$  metric,  $1 \leq p \leq \infty$ , is as follow: given two points  $q_i$  and  $q_j$  in the plane  $R^2$  with coordinates  $q_i(x_i, y_i)$  and  $q_j(x_j, y_j)$ , the distance between  $q_i$  and  $q_j$  is defined as:

$$d_p(q_i, q_j) = (|x_i - x_j|^p + |y_i - y_j|^p)^{1/p}, \quad 1 \leq p \leq \infty.$$

F.K.Hwang [10] gave an algorithm for constructing the Voronoi diagram in  $L_1$  metric in  $O(n \log n)$  time. D.T.Lee and C.K.Wong [20] presented an algorithm for  $L_1$  and  $L_\infty$  metrics in  $O(n \log n)$  time, and proved that the Voronoi diagram in  $L_\infty$  could be transferred linearly into  $L_1$  metric. Later, D.T.Lee [17] also

presented an algorithm for  $L_p$   $1 \leq p \leq \infty$  metric in  $O(n \log n)$  time. P.Chew and R.Drysdale [4] generalized  $L_p$ -metric to convex distance functions and produced an  $O(n \log n)$  time and  $O(n)$  space algorithm for constructing the corresponding Voronoi diagram. All the above mentioned algorithms use the divide-conquer method.

## Voronoi Diagrams and Convex Hulls

Brown [3] was the first one to show a linkage between Voronoi diagrams and convex hulls. By using a geometric transformation technique named *inversion*, the problem of constructing a planar Voronoi diagram for a  $n$  point set can be transferred to the problem of constructing the convex hull of  $n$  points in 3-dimensional space. The result can be generalized to the higher-dimensional space. Specifically, the Voronoi diagram of a set  $S$  in  $R^d$  ( $d$ -dimensional space) corresponds to the convex hull of  $f(S)$  in  $R^{d+1}$  through an inversion transform  $f$ .

## Other Generalizations of Voronoi Diagram

**The Voronoi Diagram of a Set of Objects other than Points** The Voronoi diagram can be generalized in many ways. For instances, the sites can be polygons, circles or other geometric figures rather than points.

R.L.Drysdale,III and D.T.Lee [6] presented an  $O\left(Nc\sqrt{\log n}\right)$  algorithm for constructing the Voronoi diagram for circles and line segments in  $R^2$ , Three years later, they presented a better result, that is  $O\left(N(\log N)^2\right)$  [5]. This result was improved to  $O(n\log n)$  by Kirkpatrick [12].

Imai et al [11] extended the ordinary Euclidean geometry for  $n$  points to the one in the Laguerre geometry for  $n$  circles in the plane, where the distance between a circle and a point is defined by the length of the tangent line from that point to the circle. They presented an  $O(n\log n)$  time and  $O(n)$  space algorithm using the divide-conquer method. The Voronoi diagram in the Laguerre geometry can be used in determining if a point belongs to the union of  $n$  circles, finding the connection of  $n$  circles, and finding the contour of the union of  $n$  circles.

**Higher-order Voronoi Diagrams (in a Plane)** For the ordinary Voronoi diagram, each polygon is the locus of points nearest to one point (order-1). The higher-order diagrams consider the  $k$  sites which are closest to a query point. It can be used for interpolation, contouring, and classification.

The definition of the generalized Voronoi polygon  $V(T)$  of a subset  $T$  of points is:

$$V(T) = \{p : \forall v \in T \ \forall w \in S - T, \ d(p, v) < d(p, w)\}$$

We can see that each point of the subset  $T$  is closer to  $p$  than the points not in  $T$ . For some  $T$ ,  $V_k(T)$  may be empty. If one lets  $k$  become  $n-1$ , one obtains the farthest point Voronoi diagram. D.T.Lee [16] presented an  $O(k^2 n \log n)$  time algorithm. Edelsbrunner, O'Rourke, and Seidel [7] gave an  $O(n^3)$  method for constructing the family of all higher-order Voronoi diagrams in  $R^d$ .

The farthest neighbor Voronoi diagrams (order-( $n-1$ ) Voronoi diagram) for  $n$  points can be constructed in  $O(n \log n)$  time [13, 26] and has been used to solve the diameter problem.

**Weighted Voronoi Diagrams** In a weighted Voronoi diagram, every point is associated with a positive weight. Each polygon of a weighted Voronoi diagram is the locus of points whose weighted distance to a given point (site) is minimum [1]. Aurenhammer gave an  $O(n^2)$  algorithm for constructing a multiplicative weighted Voronoi diagram.

**Voronoi Diagram in High Dimensions** Preparata found out that a Voronoi diagram in  $R^3$  with  $n$  points can have  $O(n^2)$  edges [23]. As mentioned above, there exists a technique called inversion transform  $f$ , which could transform a Voronoi diagram of a set  $S$  in  $R^d$  to a convex hull of  $f(S)$  in  $R^{d+1}$  [3]. In this way we can use the convex hull algorithm to obtain a Voronoi diagram in higher dimensions [3].

**Voronoi Diagrams Involving Obstacles** C.Wang and L.Seubert [34], R.Seidel [24], and A.Lingas [21] considered constrained Voronoi diagrams with obstacles and presented  $O(n \log n)$  time and  $O(n)$  space algorithm. Y.H.Tsin and C.Wang [31] gave an  $O((m+n) \log(m+n))$  algorithm ( $m$  is the number of obstacles,  $n$  is the number of sites) for constructing the geodesic Voronoi diagram  $Vor(S, O)$ , where  $O$  is a set of parallel line segments and  $S$  is a set of sites. When  $m=0$ ,  $Vor(S, O)$  goes back to the original Voronoi diagram  $Vor(S)$ . Their algorithm uses a left to right sweep and right to left sweep to build the geodesic Voronoi diagram.

## Section 2 Techniques for Constructing the Voronoi Diagram

The lower bound for constructing a Voronoi diagram on  $n$  points in the plane must take  $\Omega(n \log n)$  time and  $\Omega(n)$  space [29].

A *brute-force method* to construct a Voronoi diagram is to construct its polygons one at a time. Each polygon is the intersections of  $n-1$  half-planes if  $n$  is the number of sites in the plane, and it can be constructed in  $O(n \log n)$  time [29]. So the total time needed to construct the Voronoi diagram is  $O(n^2 \log n)$ .

### The Incremental approach

The incremental algorithms are relatively simple which construct the Voronoi diagrams by adding a site at a time, and has worst-case time complexity  $O(n^2)$  [9].

## Divide-conquer approach

Shamos and Hoey [27] used a divide-conquer method to construct the Voronoi diagram in  $O(n \log n)$  time and  $O(n)$  space where  $n$  is the number of the sites of a set  $S$  in the plane. We briefly outline the algorithm below:

1. Partition the set  $S$  into two subsets  $S_L$  and  $S_R$  with approximately equal size according to the x-coordinate.
  2. Recursively constructs  $Vor(S_L)$  and  $Vor(S_R)$ .
  - 3.1 Find the polygonal chain  $T$  which separates  $Vor(S_L)$  and  $Vor(S_R)$ .
  - 3.2 The edges of  $Vor(S_L)$  located at the right side of polygonal chain  $T$ , and the edges of  $Vor(S_R)$  located at the left side of polygonal chain  $T$  are deleted.
- The remainder is the Voronoi diagram of the set  $S$ .

Figure 1 is a set of sites in a plane which is divided into two approximately equal subsets.

Figure 1 A set of sites in a plane is divided into two approximately equal parts

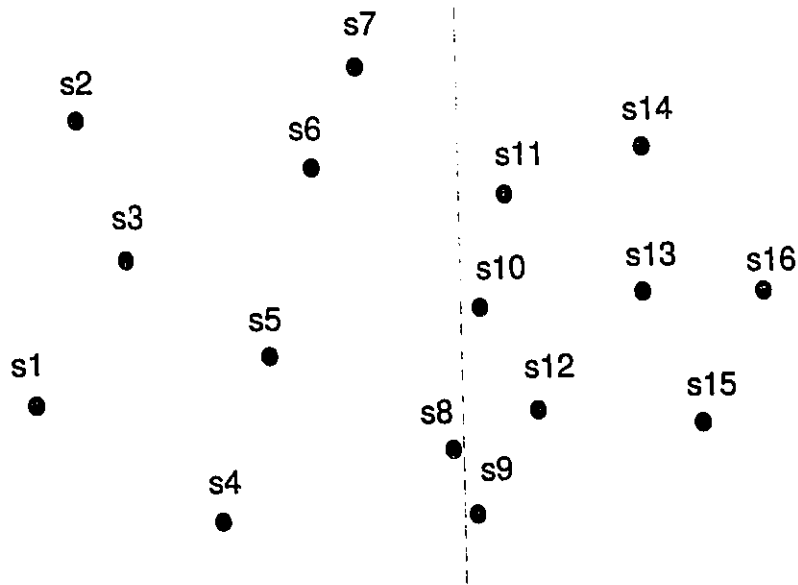
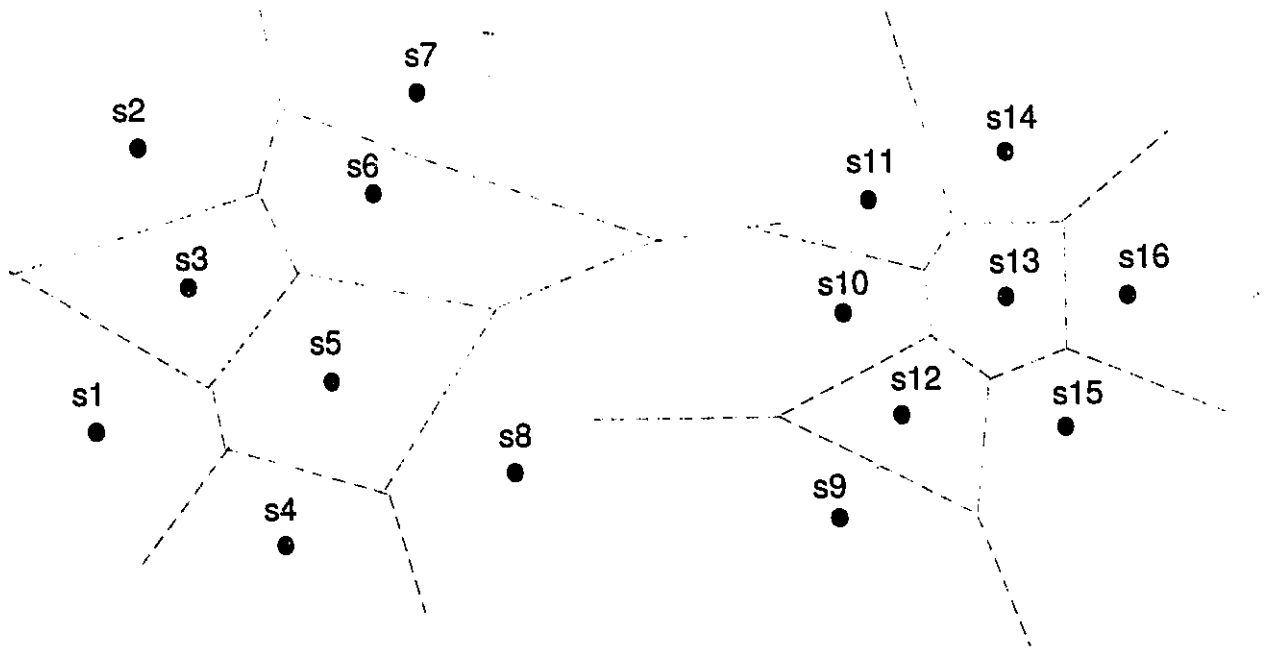


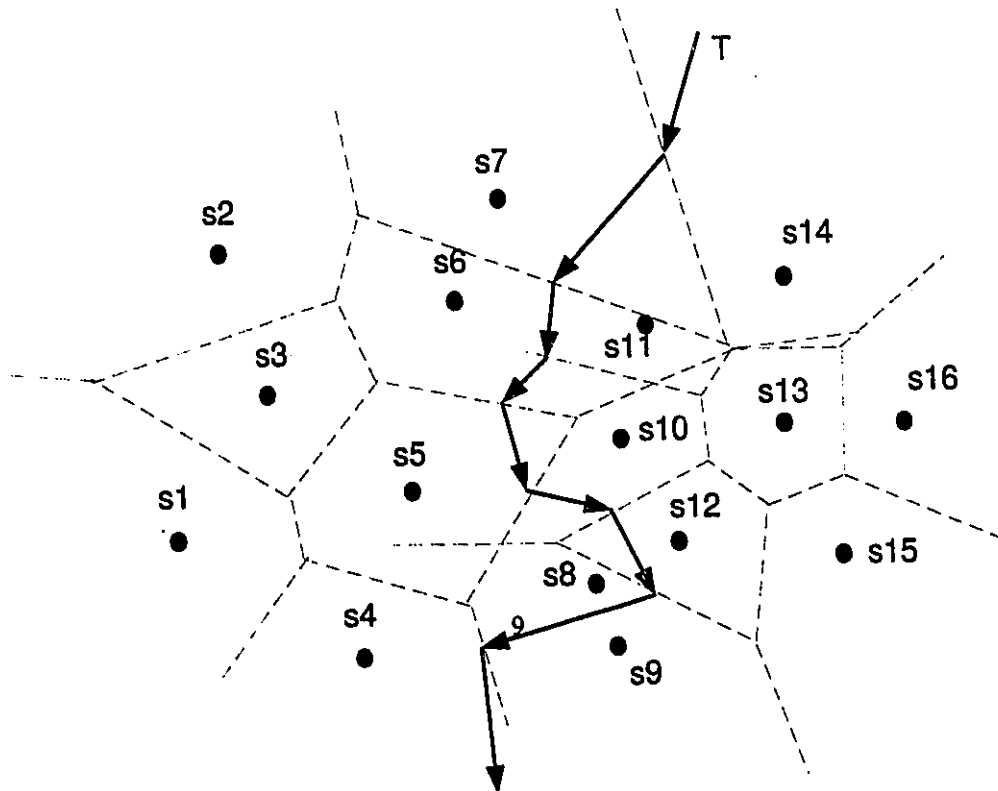
Figure 2 shows how the left Voronoi diagram  $Vor(S_L)$  and the right Voronoi diagram  $Vor(S_R)$  are merged into one by constructing the polynomial chain  $T$ .

Figure 2 The Voronoi diagram of the left subset  $Vor(S_L)$  and the Voronoi diagram of the right subset  $Vor(S_R)$  are merged into one



(a) left Voronoi diagram  $Vor(S_L)$

(b) right Voronoi diagram  $Vor(S_R)$



(c) A polygonal chain  $T$  used to merge  $Vor(S_L)$  and  $Vor(S_R)$



Step 1 and step 3.2 can be done in  $O(n)$  time. If step 3.1 can be done in  $O(n)$  time, the time complexity would be  $T(n) = 2T(n/2) + O(n) = O(n \log n)$  because of the recursive step 2.

The key point is to find the polygonal chain  $T$  which separates  $S_L$  and  $S_R$  (to merge the two parts into one) in  $O(n)$  time.

First, the two semi-infinite rays of the polygonal chain  $T$  are found: A semi-infinite ray is the perpendicular bisector of a supporting line segment of the two convex hulls  $CH(S_L)$  and  $CH(S_R)$ . Since each unbounded edge of the Voronoi diagram belongs to the perpendicular bisector of a convex hull edge, the  $CH(S_L)$  and  $CH(S_R)$  are the by-product of  $Vor(S_L)$  and  $Vor(S_R)$ . The supporting line segments of  $CH(S_L)$  and  $CH(S_R)$  can be found in linear time [27].

Then following one of the semi-infinite rays, the polygonal chain  $T$  is constructed edge by edge, until the other semi-infinite ray is reached. Each edge on  $T$  is the bisector of  $Vor(S_L)$  and  $Vor(S_R)$ . A method without backtracking is used to avoid repeatedly scanning all the edges of a Voronoi polygon when the zig-zag segments of  $T$  walk several times inside the Voronoi polygon. Therefore, the polygonal chain  $T$  can be constructed in  $O(n)$  time, the total time for constructing the Voronoi diagram is thus  $O(n \log n)$ .

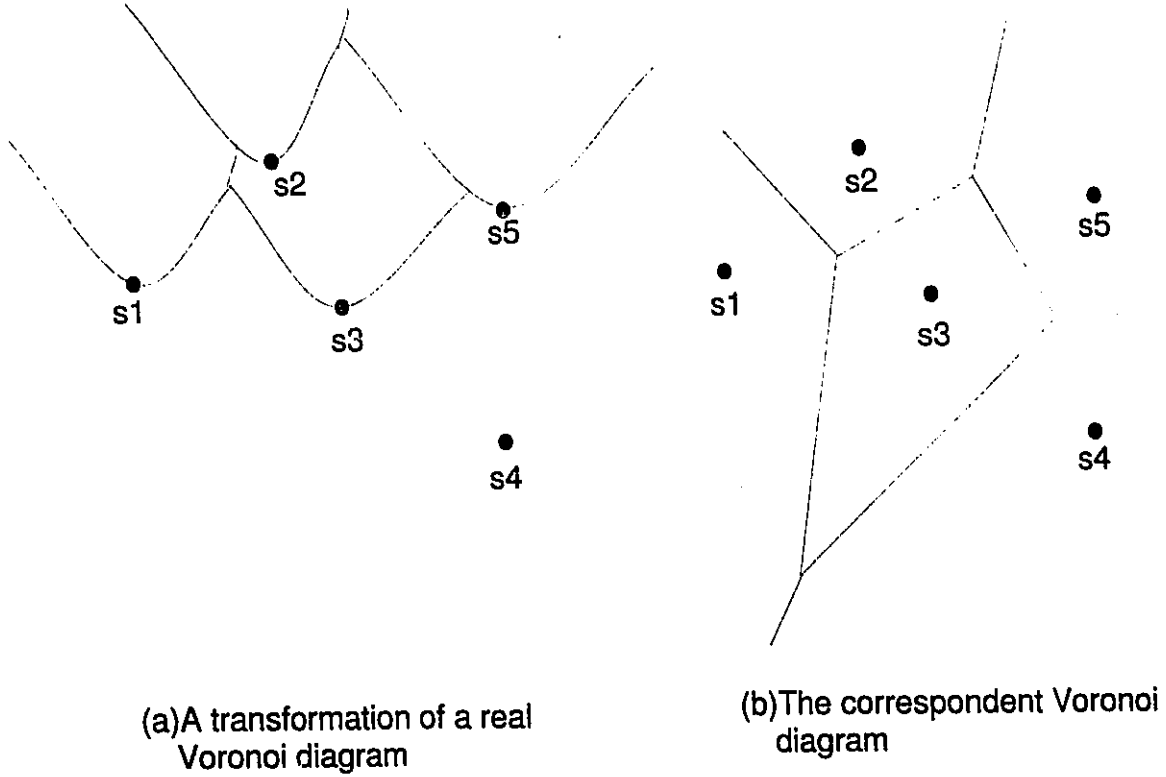
### **Sweep line approach**

Another algorithm presented by Fortune [8] used the plane sweep method

augmented with transformation to construct the Voronoi diagram in  $O(n \log n)$  time and  $O(n)$  space.

The algorithm works as follow: The plane sweep proceeds from bottom to top. Whenever a site is reached, a transformed Voronoi region for that site is built. The transformed Voronoi region has the property that its bottom-most points coincides with the site. Furthermore, the boundary of the region is computed through properly maintained information between adjacent regions along the sweep line. Then by using the same transformation, the actual Voronoi diagram can be constructed. Figure 3 (a) shows a transformed Voronoi diagram constructed by a sweep line from bottom to top. Figure 3 (b) shows the original Voronoi diagram.

Figure 3 A geometric transformation to Voronoi diagram



## Two plane sweep approach

Tsin, Y.H. and Wang, C. [31] [30] used a two plane-sweep technique to construct the geodesic Voronoi diagram  $Vor(S, O)$  for a set of sites  $S$  with a set of parallel line segments  $O$  as obstacles. Their method can be outlined as follows: The two sweeps proceeding from two opposite directions generate two data structures, called shortest-path-maps. From these two maps, for each  $p \in R^2$ , the closest site to its left and the closest site to its right can be determined.

Since the closest site of  $p$  must be one of these two closest sites, the two maps provide enough information to construct the Voronoi diagram. Tsin and Wang presented an  $O((m+n)\log(m+n))$  time  $O(m+n)$  space algorithm where  $|S|=n$  and  $|O|=m$ . When  $m=0$ ,  $Vor(S,O)$  becomes the original Voronoi diagram  $Vor(S)$ , and the time complexities are  $O(n\log n)$  and  $O(n)$  respectively.

### **A comparison of three methods**

The divide-conquer method, although elegant, has been discovered to be very difficult to implement. One of the reasons is that the assumption that the sites are in general position is difficult to remove.

Fortune's plane sweep method is elegant, and has been successfully implemented, however, good transformations for other types of Voronoi diagrams are difficult to find.

The two sweep method of Tsin and Wang avoids the use of transformation at the cost of an extra sweep.

## **Chapter 2 Voronoi Diagrams in $L_1$ and $L_\infty$ Metrics**

### **Section 1 Voronoi Diagrams in $L_1$ and $L_\infty$ Metrics**

$L_1$  and  $L_\infty$  metrics are special cases of the  $L_p$  ( $1 \leq p \leq \infty$ ) metrics (Minkowski metrics) defined as follows:

**Definition ( $L_p$  metric):** Given two points  $q_i(x_i, y_i)$  and  $q_j(x_j, y_j)$  in the plane  $R^2$ . The distance between  $q_i, q_j$ ; under the  $L_p$  ( $1 \leq p \leq \infty$ ) metrics is the distance

$$d_p(q_i, q_j) = (|x_i - x_j|^p + |y_i - y_j|^p)^{1/p} \quad (p = 1, 2, \dots, \infty).$$

Thus, the  $L_2$  metric is the conventional Euclidean metric, that is:

$$d_2(q_i, q_j) = (|x_i - x_j|^2 + |y_i - y_j|^2)^{1/2}$$

#### **$L_1$ Metric**

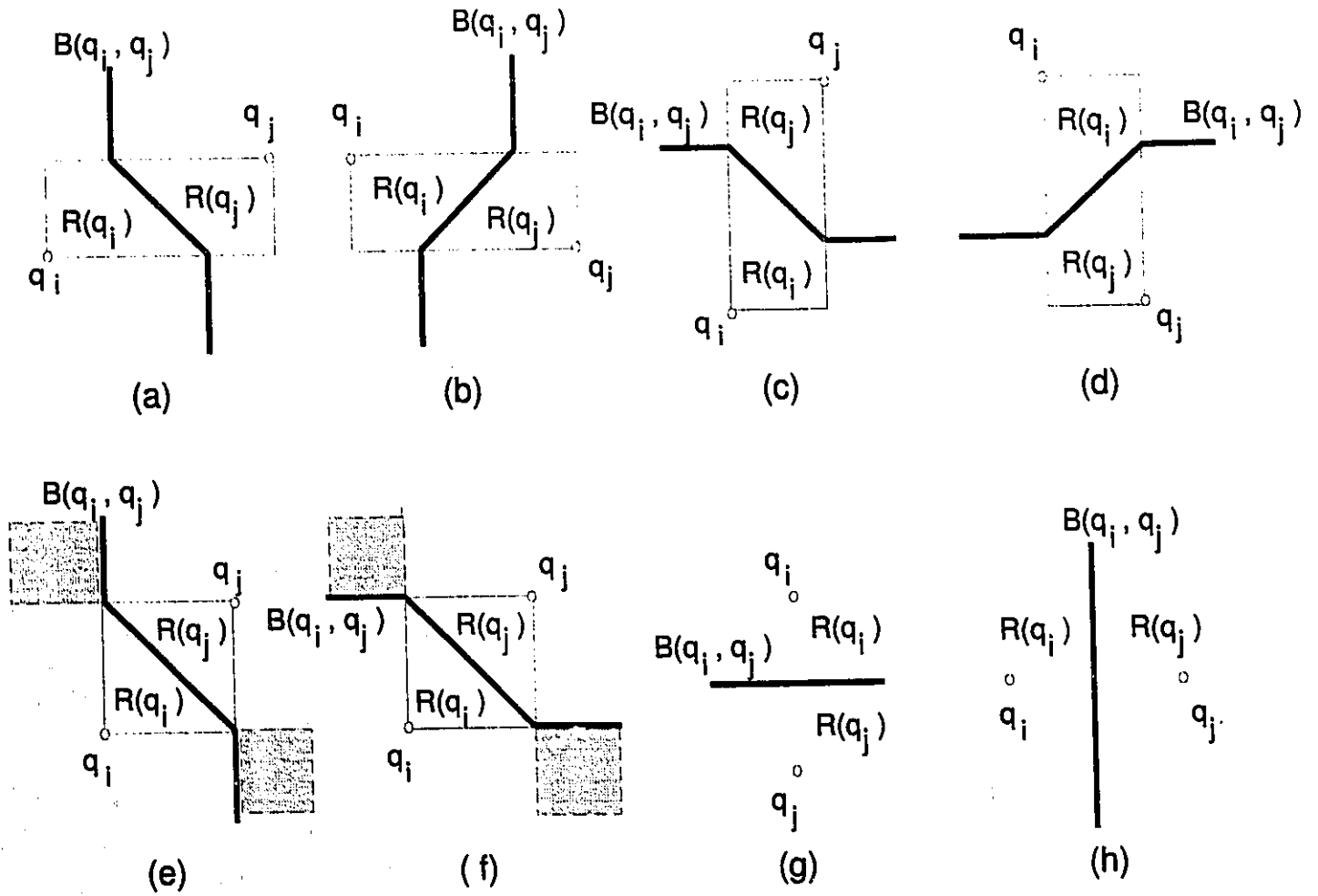
In  $L_1$  metric, the distance between points  $q_i(x_i, y_i)$  and  $q_j(x_j, y_j)$  is defined as:

$$d_1(q_i, q_j) = (|x_i - x_j| + |y_i - y_j|)$$

It is a rectilinear distance between the two points  $q_i$  and  $q_j$ . The bisector of  $q_i$  and  $q_j$ ,  $B(q_i, q_j)$ , partitions the plane into two regions,  $R(q_i)$  and  $R(q_j)$ . All the points in region  $R(q_i)$  ( $R(q_j)$  respectively) is closer to point  $q_i$  ( $q_j$  respectively) than to point  $q_j$  ( $q_i$  respectively).

Figure 4 shows the different types of bisectors of  $q_i$  and  $q_j$  that divide the plane into regions  $R(q_i)$  and  $R(q_j)$ :

Figure 4 Different types of bisectors of  $q_i$  and  $q_j$  that divide the plane into region  $R(q_i)$  and  $R(q_j)$



From figure 4 (e) and (f), we notice that part of the bisector has become a 2-dimensional region when  $|x_i - x_j| = |y_i - y_j|$ . We will adopt, for clarity, the solid

lines shown in the figure (f) as the bisector in subsequent discussion. Figure 4 (g) and (h) are the degenerate cases where the bisector becomes a horizontal line and a vertical line when  $x_i = x_j$  and  $y_i = y_j$  respectively.

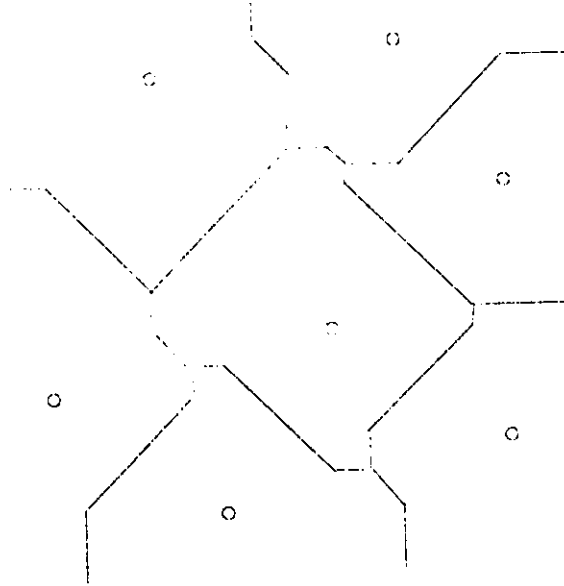
In summary, bisector consists of at most three types of segments: horizontal, vertical and  $45^\circ$  line segments.

**Definition** (Voronoi diagrams in  $L_1$  metric): Given a set  $S$  of  $n$  points  $\{p_1, p_2, \dots, p_n\}$  in the plane  $R^2$  under  $L_1$  metric, a Voronoi region (or Voronoi polygon)  $V(p_i)$  associated with a site  $p_i$  is a polygon, defined as

$$V(p_i) = \{r \in R^2 | d_1(r, p_i) \leq d_1(r, p_j), \forall j, 1 \leq j \leq n, i \neq j\}$$

Clearly, the  $n$  polygons  $V(p_i)$  ( $1 \leq i \leq n$ ) form a partition of the plane, called the Voronoi diagram of  $S$  in  $L_1$  metric, denoted by  $Vor(S)$  (figure 5). We call the intersection points of the bisectors as Voronoi points, the segments between two Voronoi points as Voronoi edges.

Figure 5 Voronoi diagram in  $L_1$  metric.



### $L_\infty$ metric

$L_\infty$  is the distance measure in plane  $R_\infty^2$ :

$$d_\infty(q_i, q_j) = \max(|x_i - x_j|, |y_i - y_j|)$$

It is well known that  $L_\infty$  can be mapped by a linear transformation from  $L_1$  metric [20]. Therefore, the construction of Voronoi diagram in  $L_\infty$  metric can be transformed to that in  $L_1$  metric.

### The Isometry of $L_1$ and $L_\infty$

Both  $L_1$  and  $L_\infty$  metrics are isometry. This can be explored as follows (figure 6): Two points  $q_i(x_i, y_i)$  and  $q_j(x_j, y_j)$  of  $R_\infty^2$  are mapped to points  $q'_i(x'_i, y'_i)$  and



$q'_j(x'_j, y'_j)$  of  $R_1^2$  respectively by the linear mapping  $f : R_\infty^2 \rightarrow R_1^2$  such that  $x'=(y+x)/2$  and  $y'=(y-x)/2$ . In figure 6, it is easily seen that the distance between  $q_i$  and  $q_j$  in  $R_\infty^2$  is

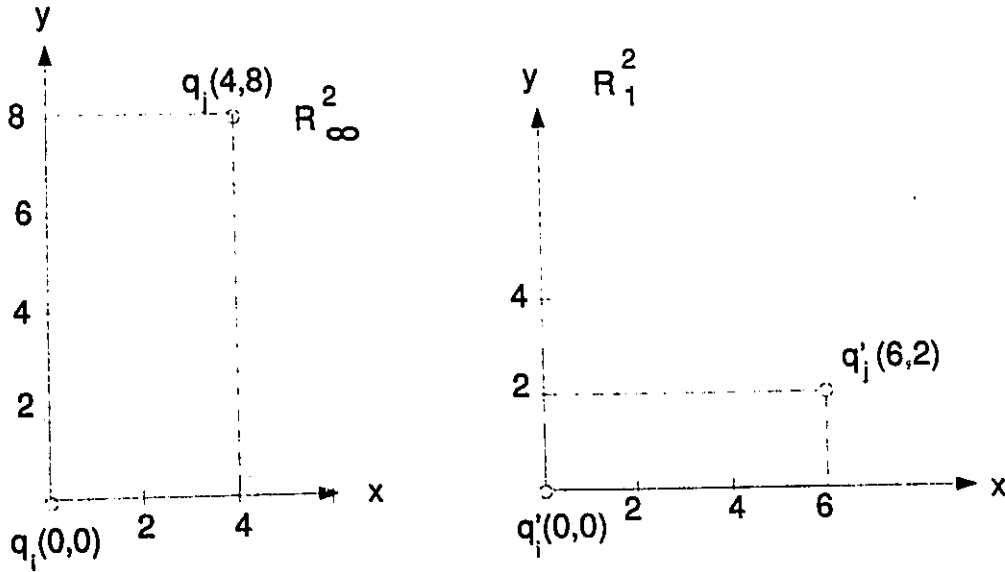
$$d_\infty(q_i, q_j) = |y_i - y_j| = 8$$

and the distance between  $q'_i$  and  $q'_j$  in  $R_1^2$  is:

$$d_1(q'_i, q'_j) = (|x'_i - x'_j| + |y'_i - y'_j|) = 8$$

Since the distant measure in  $R_\infty^2$  can be mapped to the distant measure in  $R_1^2$  and vice versa [20]. In the rest of this work we will only discuss the problems referring to  $L_1$  metric.

Figure 6 The isometry of  $L_1$  and  $L_\infty$  metrics



### The applications of $L_1$ and $L_\infty$ metrics in two-dimensional storage.

Lee and Wong [20] discovered that the Voronoi diagrams in  $L_1$  and  $L_\infty$  metrics can be used to speed up retrieval in two-dimensional storage systems.

They pointed out that for a batch of  $n$  I/O requests [2] [28], scheduling the read/write head movement to visit all the records in a two-dimensional storage system in minimum time is an open path problem (OPP). They showed that using the Voronoi diagram in  $L_1$  and  $L_\infty$  metrics, one can build a near-optimal path through each point either by constructing a minimum spanning tree or by the closest insertion method.

## Section 2 Construction the Voronoi diagram in $L_1$ and $L_\infty$ metrics by Divide and Conquer

D.T.Lee and C.K.Wong presented the divide and conquer method to construct the Voronoi diagram in  $L_1$  metric in  $O(n \log n)$  time [20]. We briefly outline the method below:

A preprocessing is needed to sort the  $n$  sites in lexicographical order.

1. Partition the set  $S$  into a left subset  $S_L$  and a right subset  $S_R$  with approximately equal size by the median x-coordinate.

2. Construct  $Vor(S_L)$  and  $Vor(S_R)$  recursively.

- 3.1 Construct the polygon line  $T$  which separates  $S_L$  and  $S_R$ .

- 3.2 Discard all edges of  $Vor(S_L)$  that lie to the right of  $T$ , and all edges of  $Vor(S_R)$  that lie to the left of  $T$ . What remains forms the Voronoi diagram  $Vor(S)$ .

The method for building the polygon line  $T$  in  $O(n)$  time is as follows:

Figure 7 is an example illustrating the *merging* process.

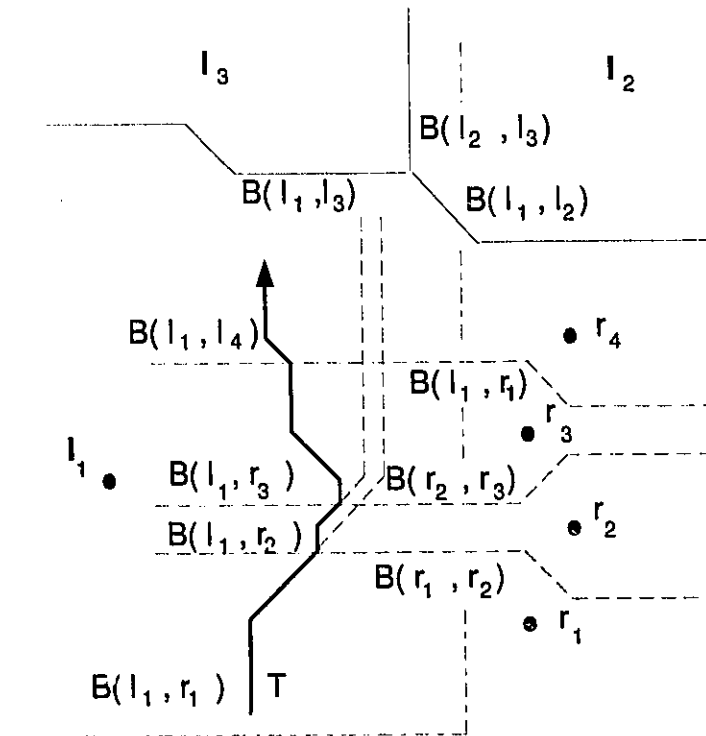
A set of 18 points with left subset  $S_L = \{1, 2, \dots, 9\}$  and right subset  $S_R = \{10, 11, \dots, 18\}$ . The left subset  $S_L$  is enclosed by the smallest rectangle which includes all the sites of the  $S_L$ . The right subset  $S_R$  is enclosed by the smallest rectangle which includes all the sites of  $S_R$ . Find the rightmost site  $w$  with the smallest index of  $S_L$ . This means that the lower right corner of the smallest rectangle of the left subset  $S_L$  is inside  $Vor(w)$ .  $\overline{wz}$  is the horizontal line segment with point  $z$  far enough to ensure intersection with the starting line

segment of the polygon line  $T$ . Find the nearest neighbor  $r$  of  $w$  among the set  $S_R$  (that is point  $10$  in  $S_R$ ). This takes  $O(n)$  time. Scan edges of  $V(10)$  to find an edge intersecting line segment  $\overline{wz}$ . In figure 7, the bisector  $B(10, 14)$  intersects  $\overline{wz}$  at  $q$ . Compare the distance between point  $w$  and point  $q$  with that between point  $w$  and point  $10$ . Since the distance between point  $w$  and  $q$  is less than the distance between point  $q$  and point  $10$ , so the bisector of point  $w$  and point  $10$  does not intersect segment  $\overline{wz}$ . Then try another point in the right subset, that is point  $14$ . The bisector of point  $w$  and point  $14$  intersects segment  $\overline{wz}$ . This is the starting line segment of the polygon line  $T$ .

The second step is to follow a zig-zag path to construct the polygonal line  $T$  until it goes out of the smallest rectangle. At any time, an imaginary point  $t$  (on the polygon line  $T$ ) always lies in two Voronoi polygons, one is in  $Vor(S_L)$ , the other is in  $Vor(S_R)$ . Whenever a new Voronoi point is created, the polygon line  $T$  will enter a new Voronoi polygon, and has a new direction. By scanning the boundary of  $V(i)$  in  $Vor(S_L)$  and  $V(j)$  in  $Vor(S_R)$ , the next point can be determined. Sometimes, polygon line  $T$  will remain inside a polygon  $V(i)$ , turning many times before crossing an edge of  $V(i)$ . In this case, we need not to scan all the edges of  $V(i)$  each time (otherwise, this procedure will take as much as quadratic time). A method without back tracking is used to save time. Figure 8 illustrates the polygon line  $T$  penetrating into  $V(i)$ , meeting the edges  $V(r_1)$ ,  $V(r_2)$ ,  $V(r_3)$ , and  $V(r_4)$  with counterclockwise turning without scanning all the  $V(i)$  edges each time.

Thus the total number of edges visited in constructing the polygon line  $T$  is proportional to the number of bisectors plus the number of Voronoi points on  $T$ . Both of them are  $O(n)$ . The merge process therefore takes  $O(n)$  time. Hence, the total time required to construct the Voronoi diagram of  $n$  sites is  $O(n \log n)$ , which is optimal in the worst case.

Figure 8 Tracing  $T$  in  $V(L_i)$  without backtracking.



## Chapter 3 Using Two Sweeps to Construct the Voronoi Diagrams in $L_1$ Metric

---

### Section 1 Shortest-Path-Map

In order to generate the Voronoi diagram of a set of site  $S$  in the plane  $R^2$ , we need to know the closest site of each point  $p \in R^2$ . The two plane sweep technique [31] is used here to create two data structures, called the left-to-right Shortest-Path-Map  $SPM_{\rightarrow}(S)$ , and the right-to-left Shortest-Path-Map  $SPM_{\leftarrow}(S)$ , represented by a Doubly-Connected-Edge-List (DCEL) structure [29].

From the  $SPM_{\rightarrow}(S)$  and  $SPM_{\leftarrow}(S)$ , the left closest site and the right closest site of each point  $p \in R^2$  can be determined, using these information, the closest site of the  $p$  can be determined.

The total order  $\prec$  is introduced here to sort the points in  $S$ . It is defined as  $\alpha \prec \beta$  iff  $x(\alpha) < x(\beta)$  or  $x(\alpha)=x(\beta)$  and  $y(\alpha) < y(\beta)$ , where  $x(\alpha)$ ,  $y(\alpha)$  stand for the  $x$  and  $y$  coordinates of  $\alpha$ , respectively.  $\alpha \preceq \beta$  iff  $\alpha \prec \beta$  or  $\alpha = \beta$ .

For clarity, we assume without loss of generality that no two or more sites have the same  $x$ -coordinate.

**Definition:** Let  $S$  be a set of sites in the plane  $R^2$ . The Left-to-Right Shortest-Path-Map of a set of sites  $S$  in the plane  $R^2$  is a set of regions

$\{\Delta(s_i) | s_i \in S, 1 \leq i \leq n\}$  such that region  $\Delta(s_i)$  is the locus of the point  $p$  such that:

i)  $x(s_i) \leq x(p)$ ;

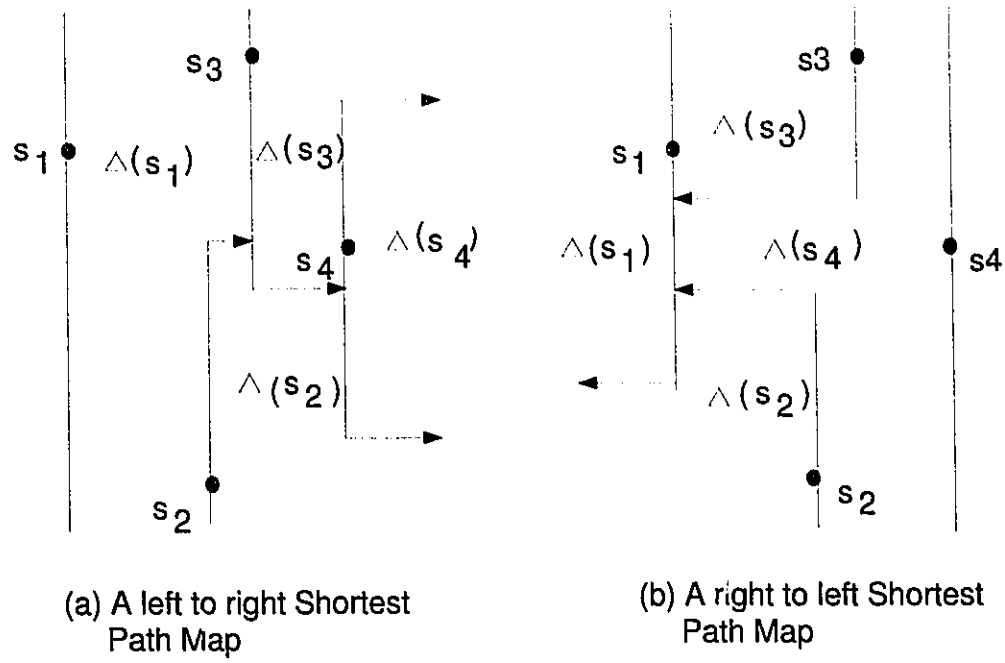
ii)  $s_i$  is the left closest site of point  $p$  among all the sites  $s'$ , no lying to the right of  $s_i$ , i.e.,

$$d_1(s_i, p) \leq d_1(s', p) \quad \forall s', x(s') \leq x(p)$$

**The Right-to-Left Shortest-Path-Map** of a set of sites  $S$  in the plane  $R^2$  can be defined in the similar way.



Figure 9 A left-to-right shortest-path-map and a right-to-left shortest-path-map



**Definition:**

The edges in a Shortest-Path-Map are called SPM arcs. The horizontal segments (part of the bisectors) are called horizontal SPM arcs (h\_SPM arcs) which sit at the same side of their two sites. The starting point of a h\_SPM arc is the corner of the region of a site. The ending point is at (1) infinity or (2) on the vertical boundary of a site. The vertical segments (sweep line or part of the sweep line) are called vertical SPM arcs (v\_SPM arcs).

**Section 2 The Construction of Shortest-Path-Map (SPM)**

To construct the  $SPM_{\perp}(S)$  ( $SPM_{\lrcorner}(S)$  respectively), a preprocessing is needed to sort all the sites  $s_i \in S (1 \leq i \leq n)$  in lexicographical order  $\prec$ . The construction will start from the leftmost site  $s_l$  and terminate after passing through the rightmost site  $s_h$ .

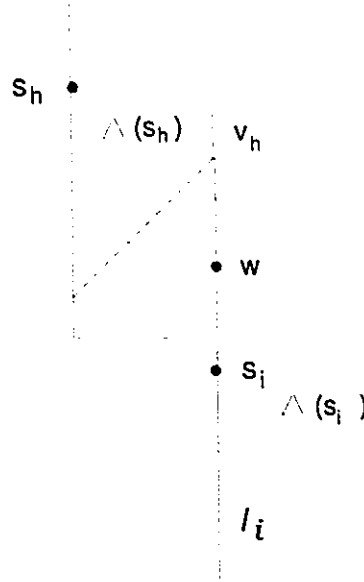
**Lemma 3.1** Let  $s_i \in S$ , and the sweep line is positioned at site  $s_i$ . Let  $v_h$  be a point on  $l_i$  such that  $v_h \in \Delta(S_h)$  where  $s_h \in S$ . Then

$$d_1(s_i, v_h) \leq d_1(s_h, v_h) \Rightarrow d_1(s_i, w) < d_1(s_h, w) \quad \forall w \in \overline{s_i v_h} - \{v_h\}$$

*Proof:*

$$\begin{aligned} d_1(s_i, w) + d_1(w, v_h) &= d_1(s_i, v_h) \leq d_1(s_h, v_h) < d_1(s_h, w) + d_1(w, v_h) \\ \Rightarrow d_1(s_i, w) &< d_1(s_h, w) \quad \blacksquare \end{aligned}$$

Figure 10  $d_1(s_i, w) < d_1(s_h, w)$

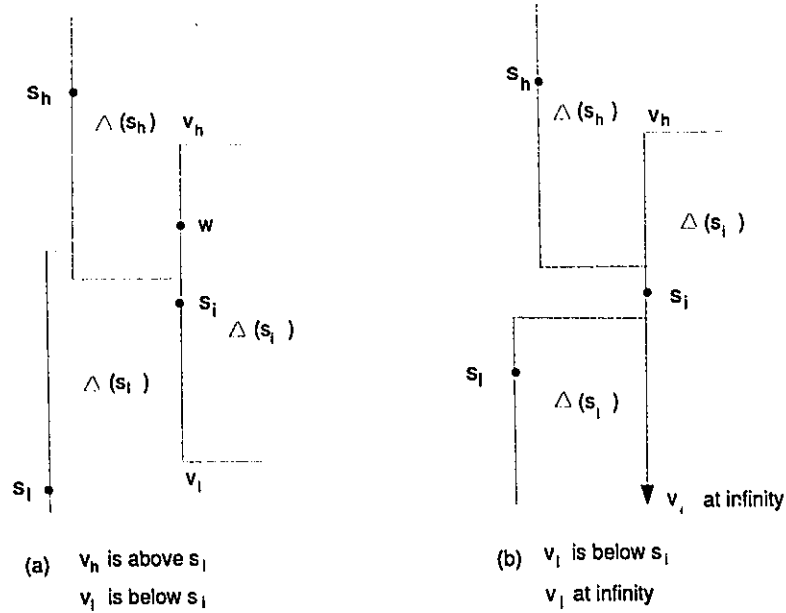


**Lemma 3.2** Let  $s_i \in S$ , the initial region of  $\Delta(s_i)$  is bounded on the left by the line segment  $\overline{v_h v_l}$  where  $v_h$  ( $v_l$ , respectively) is a point above (below, respectively)  $s_i$  such that either  $v_h$  ( $v_l$ , respectively) is at infinity or  $v_h \in \Delta(s_h)$  ( $v_l \in \Delta(s_l)$ , respectively) such that  $d_1(s_h, v_h) = d_1(s_i, v_h)$  ( $d_1(s_l, v_l) = d_1(s_i, v_l)$ , respectively).

In the latter case,  $\Delta(s_i)$  is bounded above ( below, respectively) by a bisector between  $s_i$  and  $s_h$  ( $s_l$ , respectively).

*Proof:* The lemma follows from lemma 3.1 ■

Figure 11 The upper boundary and lower boundary of an initial region  $\Delta(s_i)$



**Definition:** The point  $v_h$  is called the upper corner of  $\Delta(s_i)$  and point  $v_h$  is called the lower corner of  $\Delta(s_i)$ .

It is clearly seen that all the bisectors in  $SPM_{\rightarrow}(S)$  and  $SPM_{\leftarrow}(S)$  are horizontal line segments, so that they are monotone with respect to the x-axis.

Some data structures we used here are listed below:

- a) Queue
- b) Balanced Binary Searching Tree
- c) Doubly-Connected-Edge-List

### **Queue (Q)**

The Queue Q stores all the sites of  $S$  in the lexicographical order  $\prec$ . The sweep treats each site as an event point. When the sweep line moves from left to right, these sites will be dequeued one by one in order starting from the leftmost site  $s_1$  to the rightmost site  $s_n$ .

### **Balanced Binary Tree (T)**

The balanced binary tree T stores all the bisectors intersected by the sweep line. The bisectors are ordered from bottom to top according to their y-coordinates. Each node of the tree stores the same information of a bisector that stored in the Doubly-Connected-Edge-List (DCEL) including the y-coordinate of the bisector,  $F_L$  (field name of left side of the bisector),  $F_R$  (field name of right side of the bisector), the coordinates of the two sites of the bisector.

### **Doubly-Connected-Edge-List**

The Doubly-Connected-Edge-List is used to store the information of a planar graph embedded in the plane [29]. Each edge of the graph is described by a list of items:

1.  $v_s$ : starting vertex.
2.  $v_e$ : ending vertex.
3.  $F_L$ : field name of left side of the edge.
4.  $F_R$ : field name of right side of the edge.

5. Field: field name to which the edge belongs
6. h\_SPM: horizontal SPM arc ( part of a bisector).
7. v\_SPM: vertical SPM arc. ( sweepline or part of the sweepline).
8. t2-v: type2 Voronoi arc (part of a bisector).
9. site (pointer):
  - a. if the edge is a vertical line segment, this item has one pointer pointing to the site through which the vertical segment passes .
  - b. if the edge is a h\_SPM (part of the bisector), this item includes two pointers pointing to two sites corresponding to this edge.

It is easy to find all the edges that enclose a certain field, or a vertex at which the edges meet.

A DCEL is represented in an edge-list form. Figure 12 is an illustration of DCEL.

### **The Construction of $SPM_{\rightarrow}(S) \quad \left( SPM_{\leftarrow}(S) \right)$**

First, the leftmost site  $s_l$  is removed from the queue  $Q$ . This effectively positions the sweep line over  $s_l$ . Starting from  $s_l$  the sweep line moves towards the right, stopping at every event point until it passes through the last (i.e. rightmost) element  $s_n$  in  $Q$ .

As the sweep line is moving from the leftmost site  $s_l$  to the right, all the information of the edges that form the  $SPM_{\rightarrow}(S)$  are recorded into the data

structure DCEL. An example below (Figure 12) shows how the  $SPM_{\perp}(S)$  is constructed and how the DCEL is formed.

Figure 12 The beginning of the  $SPM_{\perp}(S)$

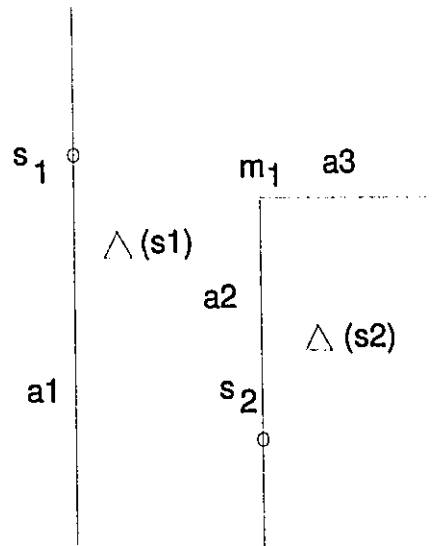


Figure 13 The corresponding DCEL represents part of the  $SPM_{\perp}(S)$ .

	$v_s$	$v_e$	$F_L$	$F_R$	$h\_SPM$	$t2\_v$	$v\_SPM$	site(ptr)
<b>a1</b>	$-\infty$	$\infty$	0	1	0	0	1	1
<b>a2</b>	$-\infty$	m1	1	2	0	0	1	2

Note that edge  $a3$  may be truncated by the other edge at later stages. The information of edge  $a3$  is now saved in the binary tree  $T$  (figure 16). It will be

saved in the DCEL only after its ending point  $v_e$  is certain (whether at  $\infty$  or truncated by a vertical edge).

At the time the sweep line stops at site  $s_3$ , the intersection point  $m3$  between the sweep line  $l_3$  and the bisector  $a3$  is found. Site  $s_3$  is in the initial region of  $\Delta(s_1)$ , the bisector of  $(s_1)$  and  $(s_3)$  has no intersection with the sweep line  $l_3$ . Therefore, site  $s_3$  is bounded above at infinity. The intersection point  $m3$  on the sweep line  $l_3$  is below site  $s_3$ . All the points on the sweep line  $l_3$  below  $m3$  is in the initial region  $\Delta(s_2)$ . The bisector of  $s_2$  and  $s_3$  has an intersection point  $m2$  on  $l_3$ . Edge  $a6$  is part of the bisector, it is a h\_SPM arc. Now,  $a4$ ,  $a5$ ,  $a6$  are added into the list, edge  $a6$  is part of the bisector of  $s_2$  and  $s_3$ . Edge  $a3$  is truncated by the sweep line  $l_3$  which passes through site  $s_3$ . Edge  $a3$  is added to the DCEL. The updated  $SPM_{\downarrow}(S)$  and DCEL are showed below. Note that the ending point of  $a6$  is uncertain at this stage, and hence cannot be saved into DCEL.



Figure 14  $SPM_{l-}(S)$  when sweep line  $l_3$  passes through  $s_3$

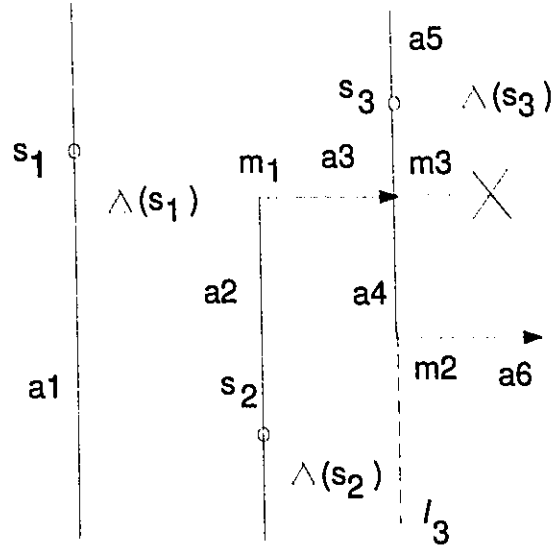


Figure 15 The corresponding DCEL represents the  $SPM_{l-}(S)$ , when sweep line passes through  $s_3$

	$v_s$	$v_l$	$F_L$	$F_R$	$h\_SPM$	$t2\_v$	$v\_SPM$	site(ptr)
<b>a1</b>	$-\infty$	$\infty$	0	1	0	0	1	1
<b>a2</b>	$-\infty$	m1	1	2	0	0	1	2
<b>a3</b>	m1	m3	1	2	1	0	0	1/2
<b>a4</b>	m2	m3	2	3	0	0	1	3
<b>a5</b>	m3	$\infty$	1	3	0	0	1	3

**Lemma 3.3** Finding the upper boundary and lower boundary of the initial region  $\Delta(s_i)$  when the sweep line is positioned at site  $s_i$  can be done in  $O(\log n)$  time.

*Proof:* At the time the sweep line is positioned at the event point  $s_i$ , the binary search tree records the order of the bisectors that intersect the sweepline from bottom to top according to their y-coordinates.

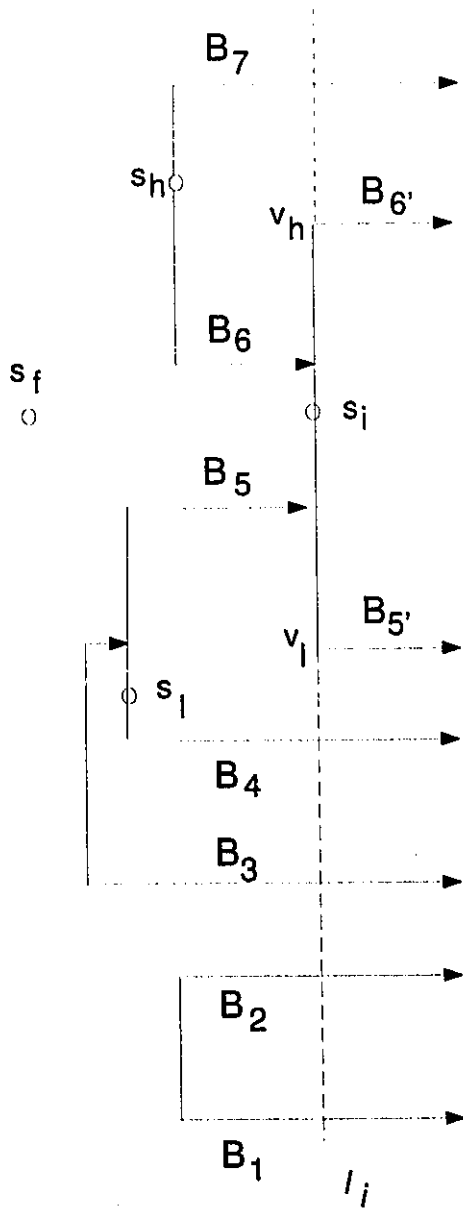
Using the y-coordinate of site  $s_i$  as the key, search T for the region  $\Delta(s_i)$  containing  $s_i$ . Then examining the bisectors above  $s_i$  (below  $s_i$  respectively) along the sweep line  $l_i$ . If no bisector above  $s_i$  (below  $s_i$  respectively) is found, that means the upper corner  $v_h$  (lower corner  $v_l$ , respectively) is at positive infinity (negative infinity respectively) of y-coordinate. Otherwise,  $v_h$  ( $v_l$ , respectively) is determined and the initial region  $\Delta(s_i)$  is bounded on the left by the line segment  $\overline{v_h v_l}$ , bounded above (below, respectively) by a h\_SPM arc originated at  $v_h$  ( $v_l$ , respectively) if  $v_h$  ( $v_l$ , respectively) exists. All the bisectors that intersect the segment  $\overline{v_h v_l}$  are truncated by  $\overline{v_h v_l}$ , and are thus deleted from the balanced binary search tree T. The newly generated bisectors are then added into T (figure 16).

*Special cases discussion:* It is possible that no bisectors (h\_SPM arcs) are met by the sweep line passing through a site. This happens: (a) at the beginning of the sweep, when the sweep line  $l_i$  is positioned at site  $s_i$ , or (b) when the vertical SPM arc passes through site  $s_i$  truncating all the bisectors and without generating a new bisector, (Figure 17 (a) and (b)). When it happens, the binary search tree T is an empty tree.

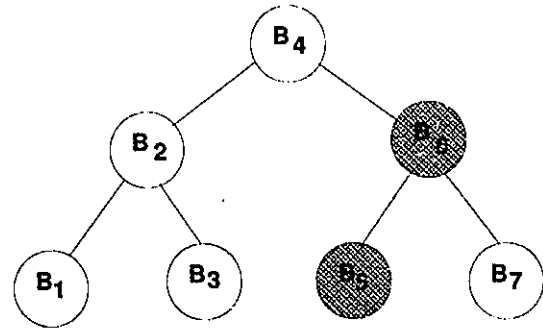
Figure 16 is an example to illustrate how to use the balanced binary searching

tree  $T$  to find the boundaries enclosing the initial region  $\Delta(s_i)$  in  $O(\log n)$  time.

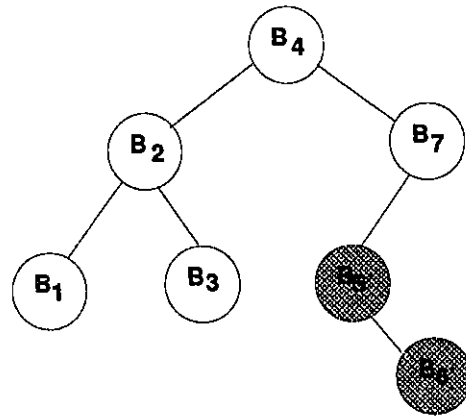
Figure 16 Using the balanced binary search tree to find the initial region  $\Delta(s_i)$  in  $O(\log n)$  time.



(a) A sweep line positioned at the site  $s_i$ , vertical segment  $\overline{v_h v_l}$  truncates the bisectors  $B_5, B_6$ .

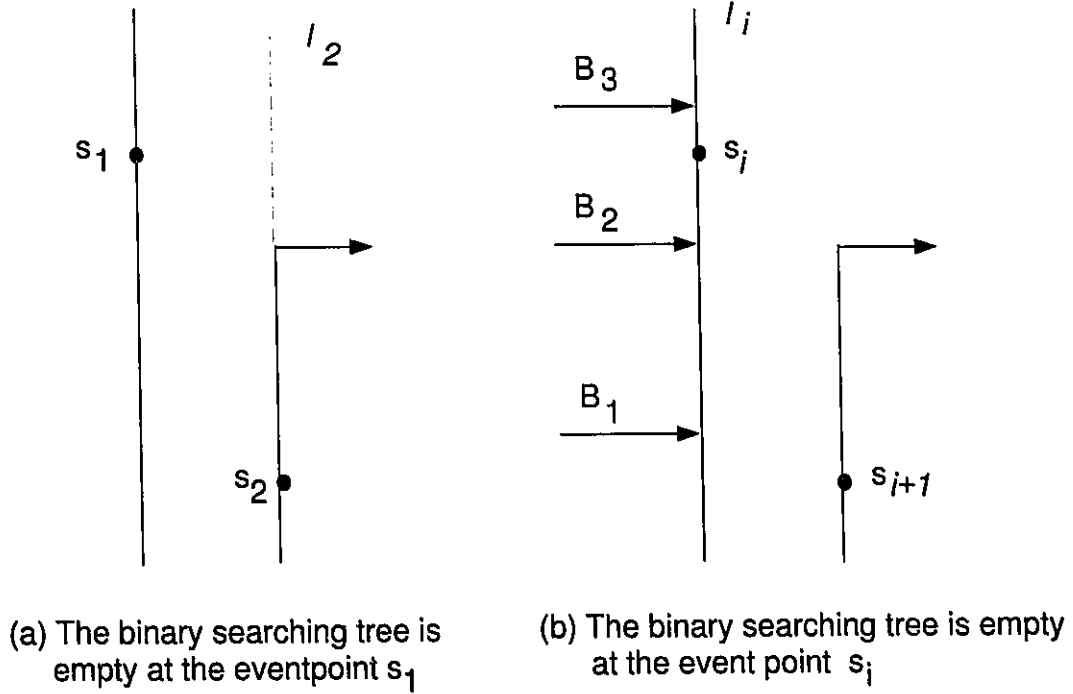


(b) A binary search tree, nodes 5 and 6 are to be deleted



(c) A binary search tree after adding nodes 5' and 6'

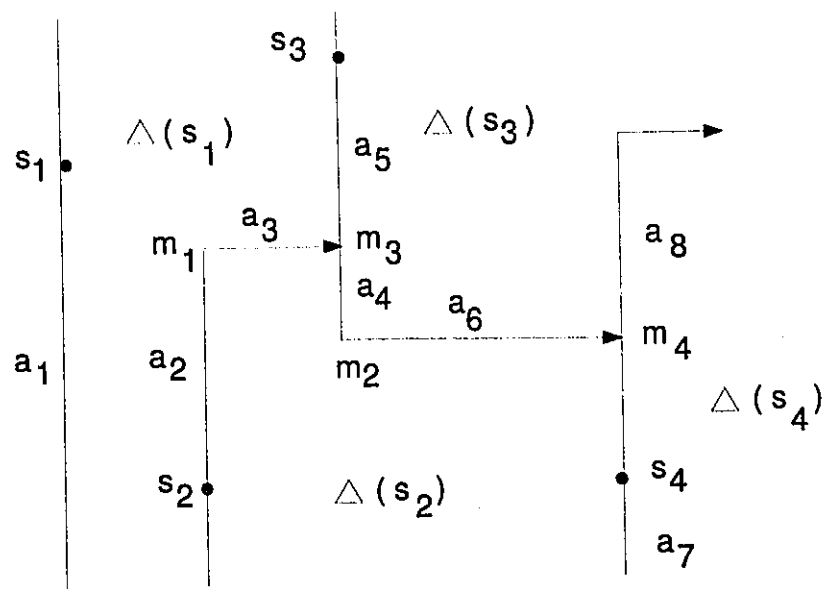
Figure 17 The balanced binary search tree  $T$  is an empty tree.



If a  $h\_SPM$  arc (part of the bisector of two sites) is truncated by  $\overline{w_h w_l}$ , the ending point of the  $h\_SPM$  arc ( the intersection between the  $h\_SPM$  arc and the segment  $\overline{w_h w_l}$ ) is fixed. This edge will be saved into the DCEL. In order to find the type 2 Voronoi arcs in each region of the plane ( this will be discussed in Section 3) efficiently, edges of  $SPM_{\perp}(S)$  in DCEL are grouped according to the fields, that is, all the edges of  $SPM_{\perp}(S)$  enclosing a certain field are grouped together. Figure 18 is an example, field  $\Delta(s_1)$  is enclosed by edges  $a1, a2, a3$ , and  $a5$ . Field  $\Delta(s_2)$  is enclosed by edges  $a2, a3, a4, a6, a7$ . Note that each

edge relates to two fields: left side field ( $F_L$ ) and right side field ( $F_R$ ) (except the edges passing through the leftmost site  $s_1$ ). Each edge (except the leftmost edge and the rightmost edge) will appear twice on the DCEL.

Figure 18 The edges enclosing one field are grouped together.



	$v_s$	$v_e$	$F_L$	$F_R$	Field	$h\_SPM$	$t2\_v$	$v\_SPM$	site(ptr)
$a_1$	$-\infty$	$\infty$	0	1	1	0	0	1	1
$a_2$	$-\infty$	$m_1$	1	2	1	0	0	1	2
$a_3$	$m_1$	$m_3$	1	2	1	1	0	0	1/2
$a_5$	$m_3$	$\infty$	1	3	1	0	0	1	3
$a_2$	$-\infty$	$m_1$	1	2	2	0	0	1	2
$a_3$	$m_1$	$m_3$	1	2	2	1	0	0	1/2
$a_4$	$m_2$	$m_3$	2	3	2	0	0	1	3
$a_6$	$m_2$	$m_4$	3	2	2	1	0	0	2/3
$a_7$	$-\infty$	$m_4$	2	4	2	0	0	1	4

The entire  $SPM_{\leftarrow}(S)$  is constructed after the sweep line passes through all the sites from left to right and the corresponding DCEL is built for later use.

*The right to left  $SPM_{\rightarrow}(S)$  can be constructed in the similar way.*

**Lemma 3.4** Constructing the Shortest-Path-Map from left-to-right  $SPM_{\leftarrow}(S)$  (right-to-left  $SPM_{\rightarrow}(S)$  respectively) of  $n$  sites can be done

in  $O(n \log n)$  time.

*Proof:* The preprocessing to sort the  $n$  sites in lexicographical order takes  $O(n \log n)$  time. It is easily verified that every edge in  $SPM_{\perp}(S)$  is (a) the leftmost vertical boundary edge of a region, or (b) the upper boundary originated at a corner, or (c) the lower boundary originated at a corner. Therefore, the total number of edges in  $SPM_{\perp}(S)$  is at most  $3n$ . As a result  $|T|=O(n)$ , and each insertion and deletion operation performed on  $T$  takes  $O(\log n)$  time. For each site  $s_i$ , finding the upper corner and lower corner of its initial region  $\Delta(s_i)$  takes  $O(\log n + k_i \log n)$  time where  $k_i$  is the number of edges truncated. since every bisector can be truncated at most once, and they are  $O(n)$  bisectors  $\sum_{i=2}^n k_i = O(n)$ . The total amount of time required to construct  $SPM_{\perp}(S)$  is thus  $O\left(n \log n + \sum_{i=2}^n k_i \log n\right) = O(n \log n)$ .

### Section 3 Constructing the Voronoi Diagram from two Shortest-Path-Maps

**Definition:** A type-1 Voronoi arc is a Voronoi arc that lies at the same side of the two sweep lines passing through the two sites which determine the arc. Obviously, every type-1 Voronoi arc is either a  $h\_SPM$  arc or a section of a  $h\_SPM$  arc.

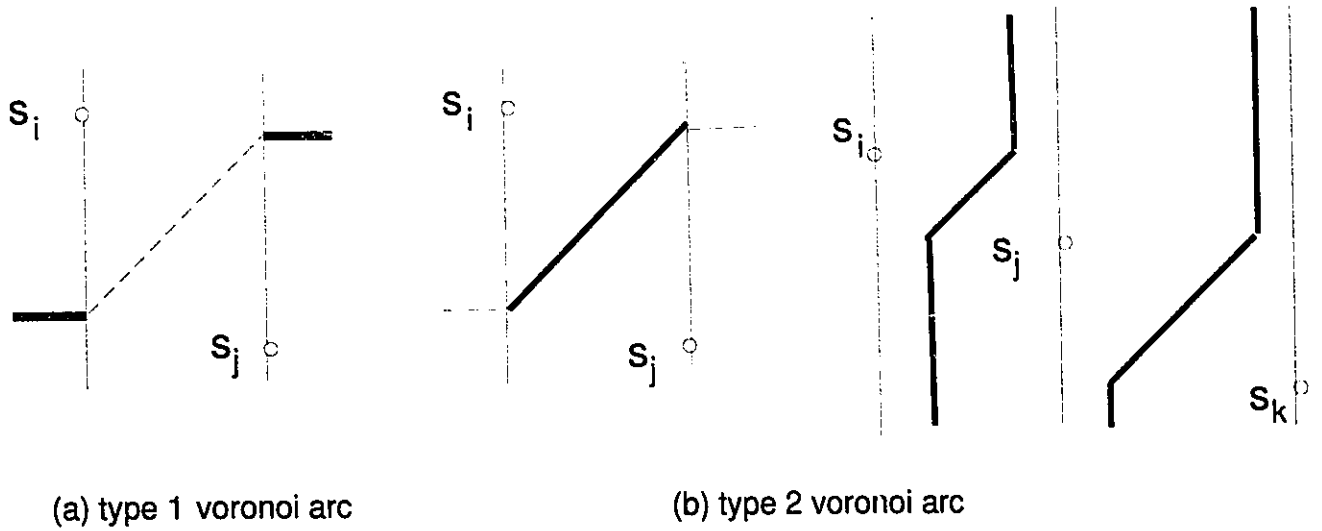
A type-2 Voronoi arc is a Voronoi arc that lies between the two sweep lines passing through the two sites determining the arc. We distinguish two cases: (1)



The Voronoi arc intersects the two sweep lines passing through its two sites, (2)

The Voronoi arc does not intersect the two sweep lines passing through its two sites.

Figure 19 Type 1 and type 2 Voronoi arcs



### Finding the type 1 Voronoi arcs

**Definition:**  $SPM_{\perp}(S)$  is the opposite SPM of  $SPM_{\lrcorner}(S)$ , and vice versa.

Entities associated with the opposite SPM are subscribed with *opp*.

#### Lemma 3.5:

Let edge  $e$  be a horizontal SPM arc (h\_SPM arc) determined by two sites  $s_i$  and  $s_j$ . Let  $u$  be a point on edge  $e$ ,  $u \in \Delta_{opp}(s_k)$  and  $d_1(s_i, u) = d_1(s_j, u) \geq d_1(s_k, u)$ . Then for any point  $p$  on edge  $e$  which is

between  $u$  and the ending part of  $e$ ,  $p \in \Delta_{opp}(s_k)$  and

$$d_1(s_i, p) = d_1(s_j, p) > d_1(s_k, p) .$$

*Proof:* Each site region is an area surrounded by vertical SPM arcs and horizontal SPM arcs. If one point on the horizontal SPM arc is in an opposite region, then every point on this horizontal SPM arc is in that opposite region. Edge  $e$  is a horizontal SPM arc, which is a section of the bisector of site  $s_i$  and  $s_j$ , and  $u$  is a point on edge  $e$  such that  $u \in \Delta_{opp}(s_k)$ , and  $d_1(s_i, u) = d_1(s_j, u) \geq d_1(s_k, u)$ . Clearly,  $u$  is equal-distant to sites  $s_i$  and  $s_j$ . Let  $p$  be a point on edge  $e$  between  $u$  and the ending point of  $e$  (that is point  $g$ ). From figure 20:

$$d_1(s_i, u) = d_1(s_j, u) \geq d_1(s_k, u)$$

$$d_1(s_i, u) = \overline{s_i c} + \overline{cu}$$

$$d_1(s_k, u) = \overline{s_k d} + \overline{du}$$

$$d_1(s_i, p) = d_1(s_i, u) + \overline{ub}$$

$$d_1(s_k, p) = d_1(s_k, u) - \overline{cb} \leq d_1(s_i, u) - \overline{cb}$$

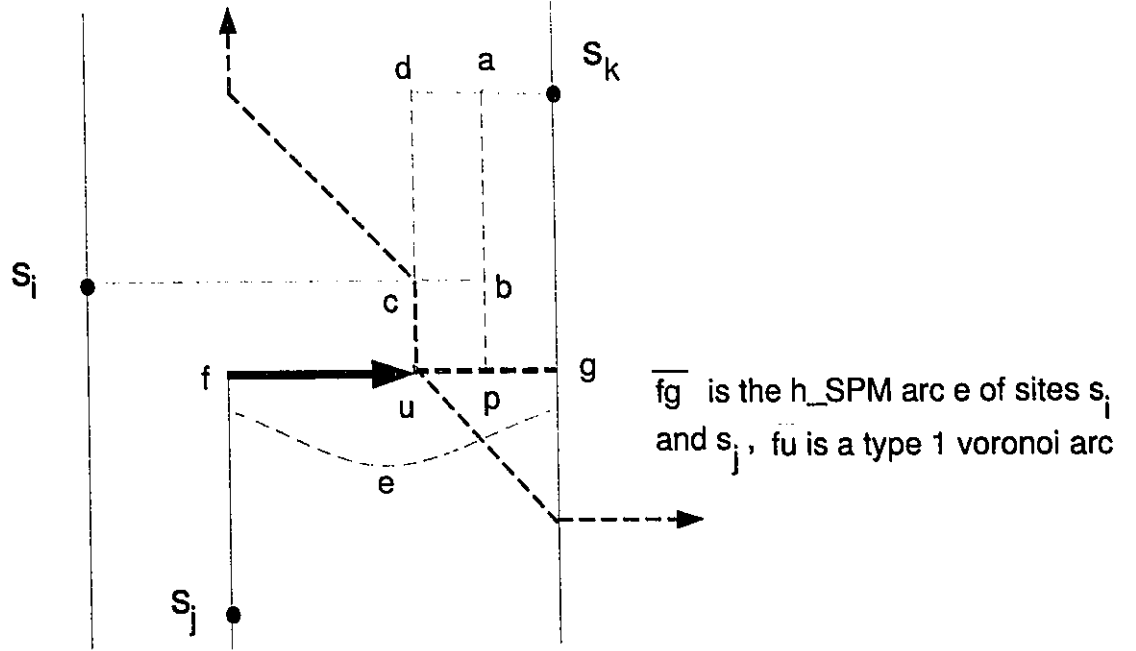
Therefore

$$d_1(s_i, p) > d_1(s_k, p)$$

Consequently

$$d_1(s_i, p) = d_1(s_j, p) > d_1(s_k, p) \blacksquare$$

Figure 20 Point  $u$  is the centre of sites  $s_i$ ,  $s_j$ , and  $s_k$ .

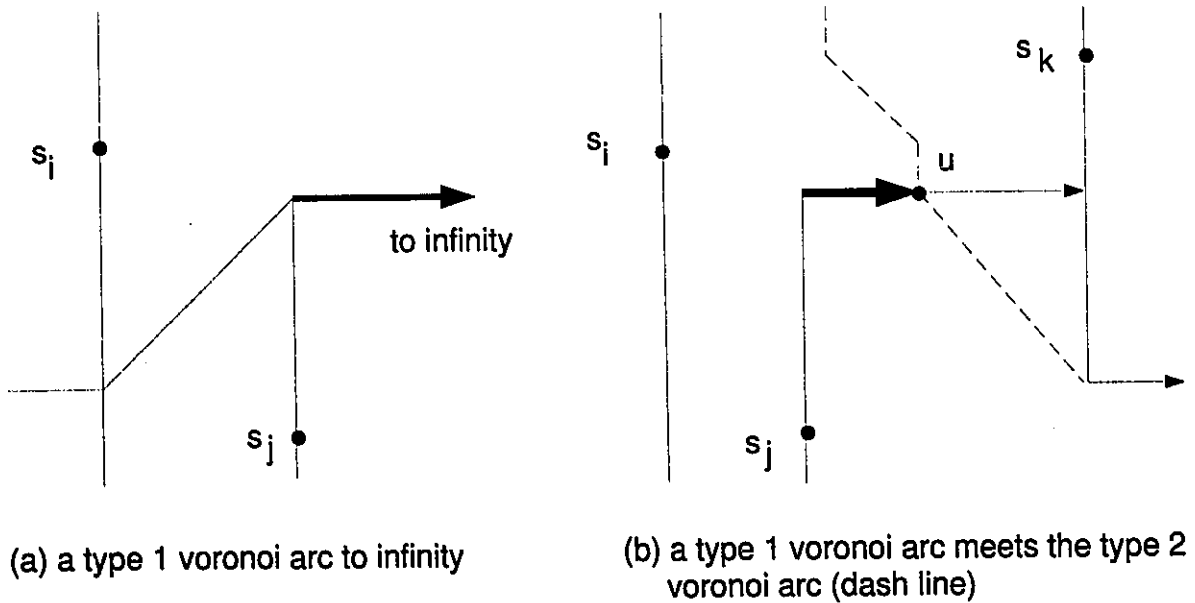


**Lemma 3.6:** The starting points of the type-1 Voronoi arc in the SPMs are the corners of the regions. The ending points of the type-1 Voronoi arcs are: (1) at infinity (figure 21(a)); (2) the intersections between  $h\_SPM$  arcs and type 2 Voronoi arcs (figure 21(b)).

*Proof:* The first statement follows immediately from the definition of the bisector in  $L_1$ -metric (figure 4). If the  $h\_SPM$  arc of the two sites does not meet the vertical line segment of any site region in the SPM, the ending point of the  $h\_SPM$  arc must end at infinity (figure 21 (a)). Obviously, the  $h\_SPM$  arc is a type-1 Voronoi arc.

If the h\_SPM arc of two sites  $s_i, s_j$  meets a type 2 Voronoi arc at a point  $u$ , the type-2 Voronoi arc must be determined by a site  $s_k$  and one of  $s_i$  and  $s_j$  (figure 21 (b)). Clearly,  $u$  is equidistant to  $s_i, s_j$  and  $s_k$ . By *Lemma 3.5*, every point lying between  $u$  and the ending point of the h\_SPM arc is closer to  $s_k$  than  $s_i$  and  $s_j$ , and every point lying between  $u$  and the starting point of the h\_SPM arc is closer to  $s_i$  and  $s_j$  than  $s_k$ . Therefore, the section of the h\_SPM arc from the starting point to  $u$  is a type-1 Voronoi arc ■

Figure 21 Type 1 Voronoi arcs



## Finding the type 2 Voronoi arcs

**Lemma 3.7:** An edge  $e$  is a type-2 Voronoi arc of sites  $s_i$  and  $s_j$  iff

$$\exists s_i, s_i \in S, e = \Delta(s_i) \cap \Delta_{opp}(s_j) \cap b(s_i, s_j) \neq \emptyset$$

where  $b(s_i, s_j)$  is the bisector of  $s_i$ , and  $s_j$ .

*Proof:*

$\Rightarrow$ ) The type-2 Voronoi arc  $e$  is a section of the bisector  $b(s_i, s_j)$  within the area  $\Delta(s_i) \cap \Delta_{opp}(s_j)$ , therefore

$$e = \Delta(s_i) \cap \Delta_{opp}(s_j) \cap b(s_i, s_j) \neq \emptyset$$

$\Leftarrow$ ) Trivial ■

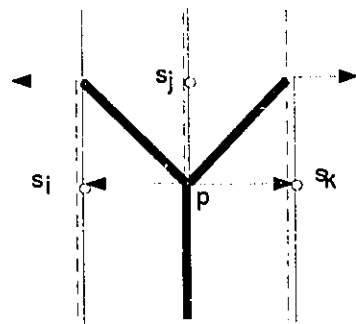
## A special case discussion:

*Three type-2 Voronoi arcs meet together.*

Case 1: Two sites  $s_i$  and  $s_k$  have the same y-coordinate, and site  $s_j$  is on the vertical bisector of site  $s_i$  and site  $s_k$ , such that  $\overline{s_i p} = \overline{s_k p} = \overline{s_j p}$  (figure 22 (a)), or  $\overline{s_i p'} = \overline{s_k p'} < \overline{s_j p'}$  (figure 22 (b)). However in (figure 22 (c)) if  $\overline{s_i p'} = \overline{s_k p'} > \overline{s_j p'}$ , the bisectors of site  $s_i$  and site  $s_j$ , the bisector of site  $s_j$  and site  $s_k$  would not meet.

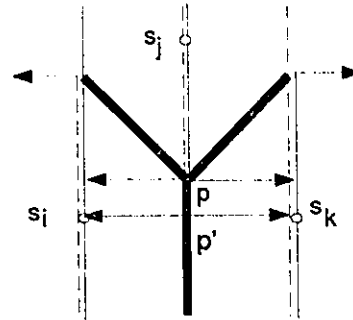
Case 2: The bisector  $\overline{ab}$  of site  $s_i$  and site  $s_j$ , the bisector  $\overline{bc}$  of site  $s_j$  and site  $s_k$  and the bisector  $\overline{bd}$  of site  $s_i$  and site  $s_k$  meet together at point  $b$  (figure 22 (d)).

Figure 22 Three type 2 Voronoi arcs meet at one point



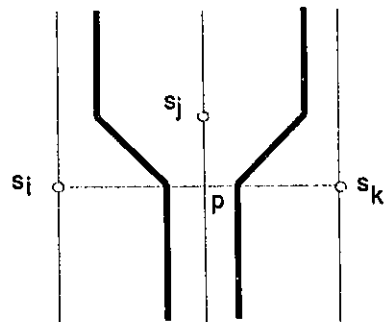
(a) Three type 2 voronoi arcs meet at point p

$$\overline{s_i p} = \overline{s_j p} = \overline{s_k p}$$



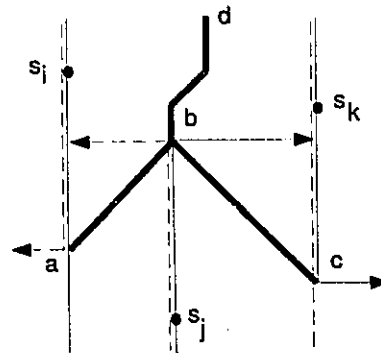
(b) Three type 2 voronoi arcs meet at point p

$$\overline{s_i p} = \overline{s_k p} < \overline{s_j p'}$$



(c) Type 2 voronoi arcs do not meet

$$\overline{s_i p} = \overline{s_k p} > \overline{s_j p'}$$



(d) Three type 2 voronoi arcs meet at point b.

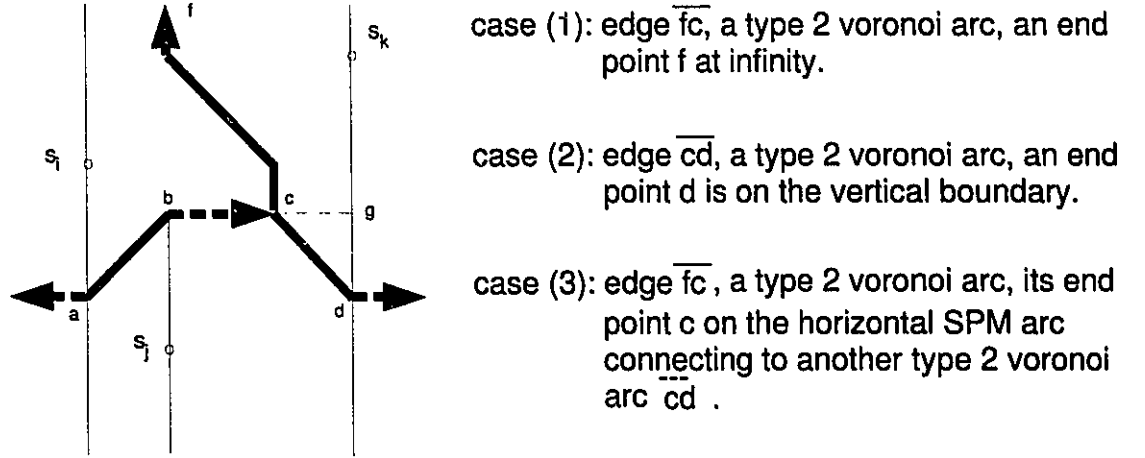
**Lemma 3.8:** Let  $e$  be a type-2 Voronoi arc such that

$$e = \Delta(s_i) \cap \Delta_{opp}(s_j) \cap b(s_i, s_j) \neq \emptyset \text{ for some sites } s_i \text{ and } s_j.$$

The end points of  $e$  are (1) at infinity; or (2) on the corners of the regions  $\Delta(s_i)$  or  $\Delta_{opp}(s_j)$ ; or (3) on the horizontal boundary of the region  $\Delta(s_i) \cap \Delta_{opp}(s_j)$ ; or (4) at the intersection of three type 2 Voronoi arcs.

*Proof:* The proof is trivial, see figure 23 for case (1), (2) and (3). See page 46 and figure 22 (a), (b), (d) for case (4) ■

Figure 23 Type 2 Voronoi arcs

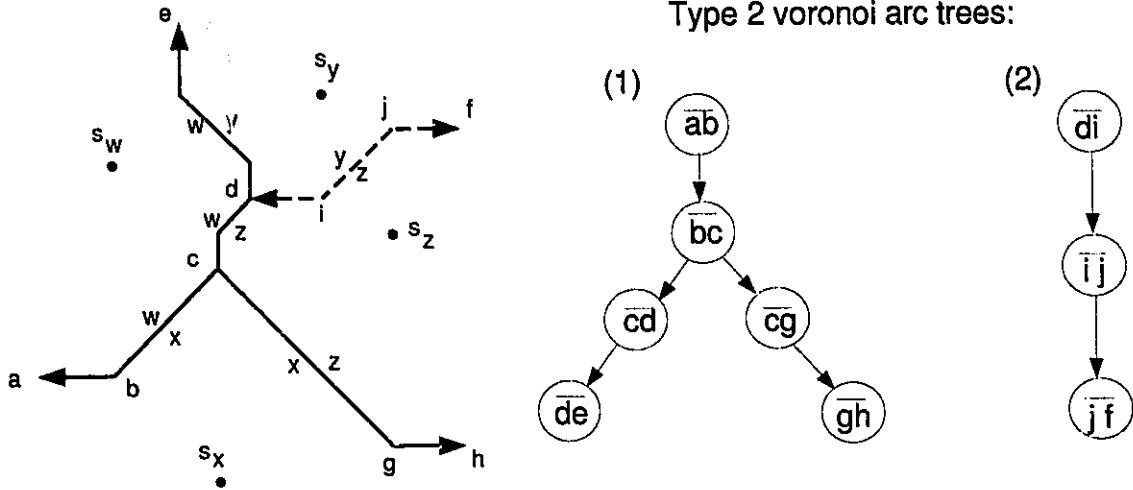


**Definition:** A type 2 Voronoi arc tree is a tree in which every internal node corresponds to a type 2 Voronoi arc and every leaf corresponds to a type-1 Voronoi arc, or a type-2 Voronoi arc which has an end point at infinity. Moreover, the Voronoi arcs in two adjacent nodes share a common endpoint.

Figure 24 shows a type 2 Voronoi arc tree. It starts from a type 1 Voronoi arc  $\overline{ab}$ , follows a type 2 Voronoi arcs  $\overline{bc}$  and then has two branches. One goes along  $\overline{cd}$ , and terminates at a type 2 Voronoi arc  $\overline{de}$ , while the other goes along  $\overline{cg}$  and terminates at a type 1 Voronoi arc  $\overline{gh}$ .

Edges  $\overline{di}$ ,  $\overline{ij}$  and  $\overline{jf}$  also form a type 2 Voronoi arc tree. It starts from  $\overline{di}$  (type 1 Voronoi arc), follows  $\overline{ij}$  (type 2 Voronoi arc) and ends at  $\overline{jf}$  (type 1 Voronoi arc).

Figure 24 Type 2 Voronoi arc tree.



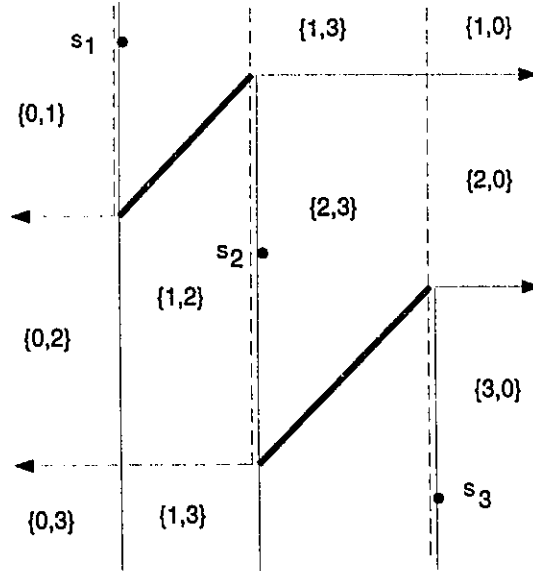
## Section 4 Algorithms

After two sweeps,  $SPM_{\rightarrow}(S)$  and  $SPM_{\leftarrow}(S)$  are constructed. An area  $\Delta(s_i) \cap \Delta_{opp}(s_j)$ ,  $s_i, s_j \in S$ , denoted by  $\{i, j\}$  is the intersection (intersections), (Figure 25  $\{1, 3\}$ ) between a left to right sweep region  $\Delta(s_i)$  and right to left



sweep region  $\Delta_{opp}(s_j)$ . Site  $s_i$  is the closest left site of every point inside area  $\{i, j\}$ , and site  $s_j$  is the closest right site of every point inside area  $\{i, j\}$ . An area  $\{i, j\}$  may be a closed area enclosed by the SPM arcs, or with some edges open at infinity. The areas located at the left side of the sweep line passing through the leftmost site  $s_l$  belong to only one region, that is area  $\{0, 1\}$ . The area located at the right side of a sweep line passing through the rightmost site  $s_n$  belong to only one region, that is area  $\{n, 0\}$ . Obviously, there is no type 2 Voronoi arc inside the areas  $\{0, 1\}$  or  $\{n, 0\}$ , which has only one closest site  $s_l$  or  $s_n$ . The horizontal boundaries of the one site area  $\{0, 1\}$  or  $\{n, 0\}$  are type 1 Voronoi arcs. Note that some areas  $\{i, j\}$  do not have the type 2 Voronoi arc inside, the bisector of site  $s_i$  and  $s_j$  do not cross through these two site areas, (figure 25).

Figure 25 Areas  $\Delta(s_1) \cap \Delta_{opp}(s_3)$  represented by  $\{1, 3\}$  have no type 2 Voronoi arcs inside.



Viewing the plane divided by the two SPMs as a collection of areas  $\Delta(s_i) \cap \Delta_{opp}(s_j)$ ,  $s_i, s_j \in S$  will help us in finding the type 1 and type 2 Voronoi arcs.

Three DCELs are used to store the information when tracing the type 2 Voronoi arc tree:

$D_{st}$ : stores the h\_SPM arcs which have one ending point at infinity and the type-2 Voronoi arcs which have one ending point at infinity as the starting edges to trace the type 2 Voronoi arc trees. The type-2 Voronoi arcs which are starting edges at the branch of the type-2 Voronoi arc tree are also stored in  $D_{st}$  (figure 24,  $\overline{cg}$  or  $\overline{cd}$ ).

$D_{end}$ : stores the h\_SPM arcs and type 2 Voronoi arcs which terminate the type 2 Voronoi arc trees.

$D_v$ : stores all the edges of the Voronoi diagram.

After the left to right sweep and the right to left sweep, we obtain two shortest-path-maps:  $SPM_{\rightarrow}(S)$  and  $SPM_{\leftarrow}(S)$ , which are represented by Doubly-Connected-Edge-List (DCEL). All h\_SPM arcs whose one ending point is at infinity and all type-2 Voronoi arcs whose one ending point is at infinity (extreme edges) are copied to two DCEL structures:  $D_{st}$  ( $D_{st}$  is a DCEL data structure for storing the extreme edges for tracing type 2 Voronoi arc trees), and  $D_v$  ( $D_v$  is a DCEL data structure for storing the Voronoi diagram).

Pick up the extreme edges one by one from  $D_{st}$ , trace back into the areas one after another to find out all the type 2 Voronoi arcs in the tree (this will be discussed later). The leaf edge of a type 2 Voronoi arc tree is a type 1 Voronoi arc which follows a type 2 Voronoi arc ended at the vertical boundary of the area, or a type 2 Voronoi arc which ended at infinity. The intersections between type 2 Voronoi arcs and h\_SPM arcs (an edge on the boundary of the area in which the type 2 Voronoi arc locates) are the heads of type 1 Voronoi arcs. These type 1 Voronoi arcs are also roots of type 2 Voronoi arc trees. Store these type 1 Voronoi arcs into  $D_{st}$  (DCEL) for later tracing. In cases where three type 2 Voronoi arcs meet together at the corners of the areas (figure 22), pick one type 2 Voronoi arc

for continuous tracing, store the other type 2 Voronoi arc into  $D_{st}$  (DCEL) for later tracing. Pick every edge stored in the  $D_{st}$  (DCEL) and trace out its type 2 Voronoi arc tree until all the edges are traced. Store every type 1 Voronoi arc and type 2 Voronoi arc of the type 2 Voronoi arc tree into  $D_v$  during the tracing.  $D_v$  is the required DCEL storing the Voronoi diagrams.

We can easily find out whether there is a type 2 Voronoi arc lying inside an area, and find out the intersections between the type 2 Voronoi arc and the enclosing edges of the area  $\{i, j\}$  by searching under the fields  $\Delta(s_i)$  and  $\Delta_{opp}(s_j)$  of DCEL which stores all the information of  $SPM_{\perp}(S)$  and  $SPM_{\leftarrow}(S)$ .

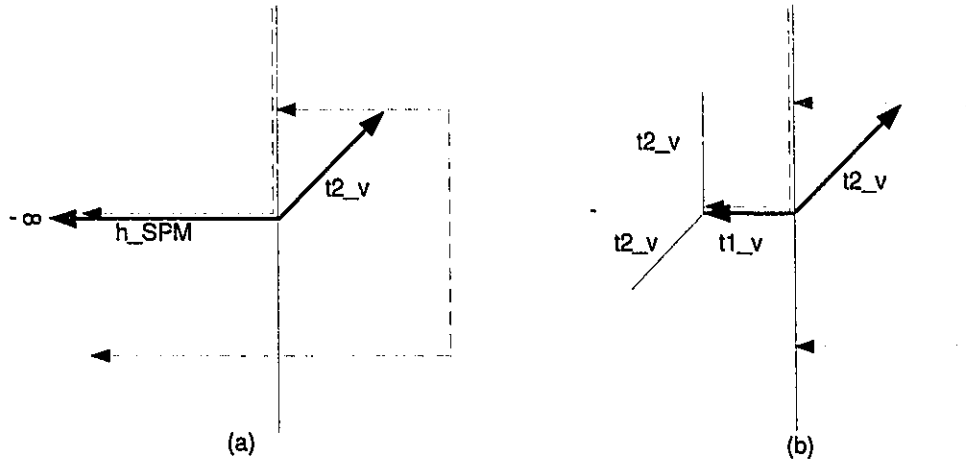
To trace back all the type 2 Voronoi arc trees, six different cases are discussed below:

*Case 1:* (figure 26) Pick up an edge from  $D_{st}$ . Regardless of whether it is a h\_SPM arc with its ending point at infinity or a type 1 Voronoi arc, its starting point is on a vertical SPM arc (v\_SPM) and will be followed by a type 2 Voronoi arc. The area in which the following type 2 Voronoi arc locates is the intersection of two fields which are the same as the left field and the right field of the previous h\_SPM arc.

When the area in which the type 2 Voronoi arc locates is known, that means the two fields are known. Get the grouped edges of field  $\Delta_{opp}(s_j)$  of the area from the DCEL, compute the type 2 Voronoi arc which is inside of the area, the starting point of the type 2 Voronoi arc is the same as the starting point of the

$h\_SPM$  arc (or the type 1 Voronoi arc). The ending point of the type 2 Voronoi arc is the intersection between the type 2 Voronoi arc and one of the edges of field  $\Delta_{opp}(s_j)$  of the area.

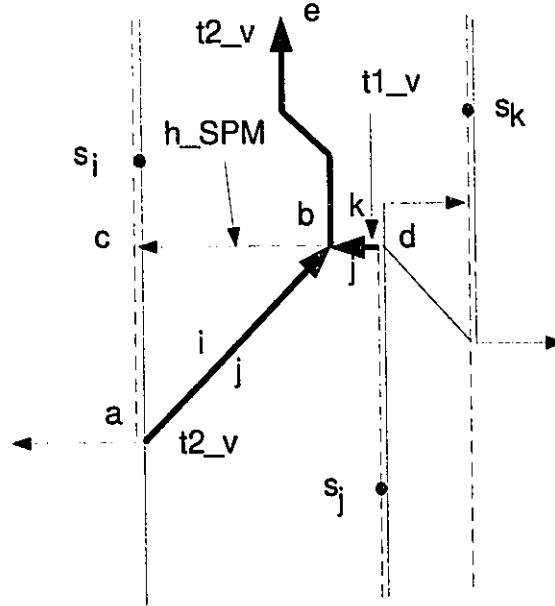
Figure 26 Start tracing back the type 2 Voronoi arc tree from (a) a  $h\_SPM$  arc with the ending point at infinity, or from (b) a type 1 Voronoi arc.



*Case 2:* (figure 27) An ending point of a type 2 Voronoi arc  $\overline{ab}$  is on a  $h\_SPM$  arc  $\overline{dc}$  which is the boundary of the opposite field  $\Delta_{opp}(s_j)$  of the area in which the type 2 Voronoi arc resides. The left (right) side field of type 2 Voronoi arc  $\overline{ab}$  is  $\Delta(s_i)$  ( $\Delta(s_j)$ ). The left (right) side of  $h\_SPM$  arc  $\overline{dc}$  is  $\Delta(s_j)$  ( $\Delta(s_k)$ ). So the next type 2 Voronoi arc  $\overline{be}$  is in the area  $\{i, k\}$ . The processing is: compute the type 2 Voronoi arc  $\overline{ab}$  in area  $\{i, j\}$ , get the ending point  $b$  of the type 2 Voronoi arc  $\overline{ab}$  ( $b$  is on a  $h\_SPM$  arc which is the boundary of the opposite field  $\Delta_{opp}(s_j)$

of area  $\{i, j\}$ , get the type 1 Voronoi arc  $\overline{db}$ , check if the h\_SPM arc  $\overline{dc}$  is in the  $D_{end}$  (DCEL). If  $\overline{dc}$  is inside  $D_{end}$ , delete  $\overline{dc}$  from  $D_{end}$ , and save type 1 Voronoi arc  $\overline{db}$  into  $D_v$ . If  $\overline{dc}$  is not in the  $D_{end}$ , store  $\overline{ab}$  into  $D_{st}$  (for later tracing) and  $D_v$ .

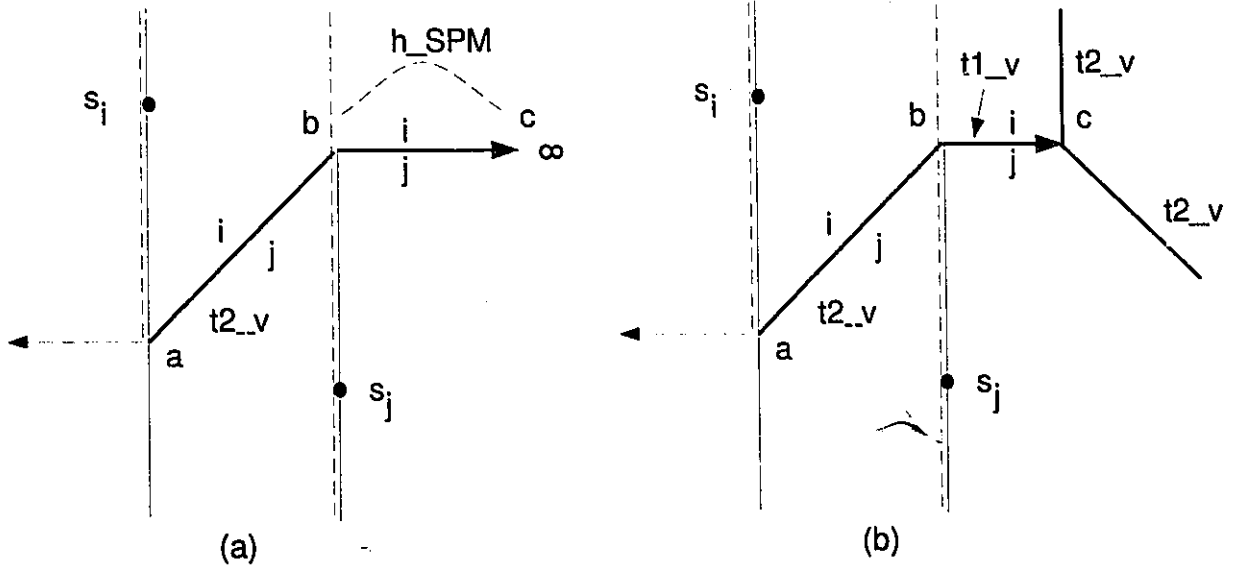
Figure 27 Tracing back from a type 2 Voronoi arc to another type 2 Voronoi arc, and meet a type 1 Voronoi arc as a root of a new type 2 Voronoi arc tree.



*Case 3:* (figure 28 (a)) At the time of tracing back along the type 2 Voronoi arc tree, if the ending point  $b$  of a type 2 Voronoi arc  $\overline{ab}$  is on the vertical boundary of the area in which the type 2 Voronoi arc locates, the next edge is a h\_SPM arc. The left side field and the right side field of this h\_SPM arc  $\overline{bc}$  is the same as the left side field and the right side field of  $\overline{ab}$ .

If the ending point of the h\_SPM arc  $\overline{bc}$  is at infinity,  $\overline{bc}$  must already exist in  $D_{st}$ , then delete it from  $D_{st}$ .

Figure 28 Tracing back from a type 2 Voronoi arc to (a) a h\_SPM arc with the ending point at infinity. (b) a type 1 Voronoi arc which is met by other type 2 Voronoi arc tree.



*Case 4:* (figure 28(b)) If the ending point  $b$  of a type 2 Voronoi arc  $\overline{ab}$  is on the vertical boundary of the area in which the type 2 Voronoi arc locates, the next edge is a h\_SPM arc  $\overline{bc}$ . The left side field and right side field of  $\overline{bc}$  is the same as the left side field and right side field of  $\overline{ab}$ . Check whether this h\_SPM arc  $\overline{bc}$  is inside the  $D_{st}$  (DCEL): (1) If it exists in the  $D_{st}$  already, it means this h\_SPM arc was intersected by another type 2 Voronoi arc tree, and  $\overline{bc}$  was saved into  $D_{st}$  before the current tracing of type 2 Voronoi arc tree along  $\overline{ab}$  and  $\overline{bc}$ . Delete it

from  $D_{st}$ , because this type 2 Voronoi arc tree has been traced by now. (2) If it doesn't exist in the  $D_{st}$ , save it in the  $D_{end}$ , it indicates that the type 2 Voronoi arc tree starting from this h\_SPM arc  $\overline{bc}$  needs not be traced again. When the h\_SPM arc  $\overline{bc}$  is intersected by the other type 2 Voronoi arc tree at point  $c$  later on, whether the type 2 Voronoi arc tree started from  $\overline{bc}$  has been traced or not can be known by checking if  $\overline{bc}$  is inside  $D_{end}$  or not.

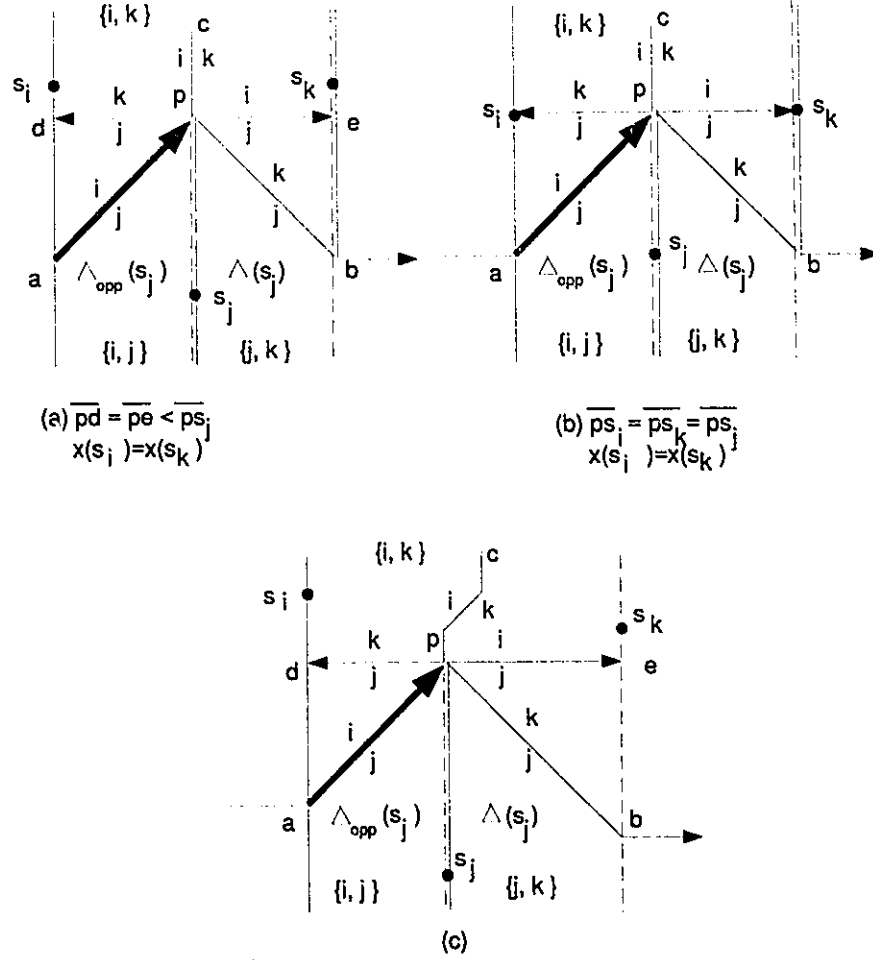
**Lemma 3.9** Let  $s_i, s_j$  and  $s_k$  be three sites in the plane. If the end point of a type 2 Voronoi arc of the area  $\{i, j\}$  is at the corner  $p$  of the area  $\{i, j\}$ , then the corner  $p$  must also be the corner of adjacent area  $\{j, k\}$ , where site  $s_j$  is on the boundary of both area  $\{i, j\}$  and  $\{j, k\}$ . If two sites  $s_i, s_k$  have the same x-coordinates, the three sites  $s_i, s_j$  and  $s_k$  are vertices of an isosceles triangle.

*Proof:* (figure 29) Let  $p$  be the corner of area  $\{i, j\}$ ,  $\overline{ap}$  be a type 2 Voronoi arc of area  $\{i, j\}$ ,  $\overline{pd}$  be a h\_SPM arc as part of the boundary of area  $\{i, j\}$ , so that the starting point  $a$  of  $\overline{ap}$  is on the vertical line passing through site  $s_i$ , the ending point  $p$  of  $\overline{ap}$  is on the vertical line passing through site  $s_j$ . According to the method of constructing the SPM, the edges  $\overline{ps_j}$  and  $\overline{pe}$  are part of the boundaries of field  $\Delta(s_j)$ . From lemma 3.6,  $\overline{pe}$  is a h\_SPM arc starting from the corner  $p$  of region  $\Delta(s_j)$  with left side field  $\Delta(s_i)$  and right side field  $\Delta(s_j)$ . According to the method of constructing the SPM,  $\overline{pd}$  and  $\overline{ps_j}$  must be part of the boundaries of field  $\Delta_{opp}(s_j)$ . Edge  $\overline{pd}$  (a h\_SPM arc) is part of the bisector of site  $s_j$  and the other site, say  $s_k$ . The left side field of  $\overline{pd}$  is field  $\Delta_{opp}(s_j)$ , the right side field of



$\overline{pd}$  is field  $\Delta_{opp}(s_k)$ .  $\overline{pe}$  and  $\overline{pd}$  are both h\_SPM arcs, and belonging to field  $\Delta(s_j)$  and field  $\Delta_{opp}(s_j)$  respectively, so that corner  $p$  is the centre of three sites  $s_i$ ,  $s_j$  and  $s_k$ . If site  $s_i$  and site  $s_k$  have the same x-coordinates, then  $s_i$ ,  $s_j$  and  $s_k$  are three vertices of an isosceles triangle, and  $|x(s_i) - x(s_j)| = |x(s_j) - x(s_k)|$ ,  $y(s_i) = y(s_k)$ , (figure 29 (a) (b)). If site  $s_i$  and site  $s_k$  have different x-coordinates, then the situation is depicted in figure 29 (c) ■

Figure 29 Three type 2 Voronoi arcs meet together.



**Case 5:** (figure 29(a)) If the ending point of a type 2 Voronoi arc  $\overline{ap}$  is on the corner of the area  $\{i, j\}$  in which the type 2 Voronoi arc  $\overline{ap}$  resides. From *lemma 3.9*,  $p$  is equidistant to the three sites. Check from  $D_{st}$  if the edge  $\overline{ap}$  is already recorded inside, that is, check if two type 2 Voronoi arcs  $\overline{bp}$  and  $\overline{pc}$  are traced in the other type 2 Voronoi arc tree already. If it is inside  $D_{st}$ , delete edge  $\overline{ap}$  from

$D_{st}$ . Otherwisw, do the following: get the h\_SPM arc  $\overline{pd}$ , find out the left and right field of  $\overline{pd}$ , that is  $\Delta_{opp}(s_j)$  and  $\Delta_{opp}(s_k)$ . Then the neighboring area of area  $\{i, j\}$  will be area  $\{j, k\}$  and area  $\{i, k\}$ . Compute the type 2 Voronoi arcs in both area  $\{j, k\}$  and area  $\{i, k\}$ , save one type 2 Voronoi arc in  $D_{st}$  for later tracing, and trace back along another type 2 Voronoi arc.

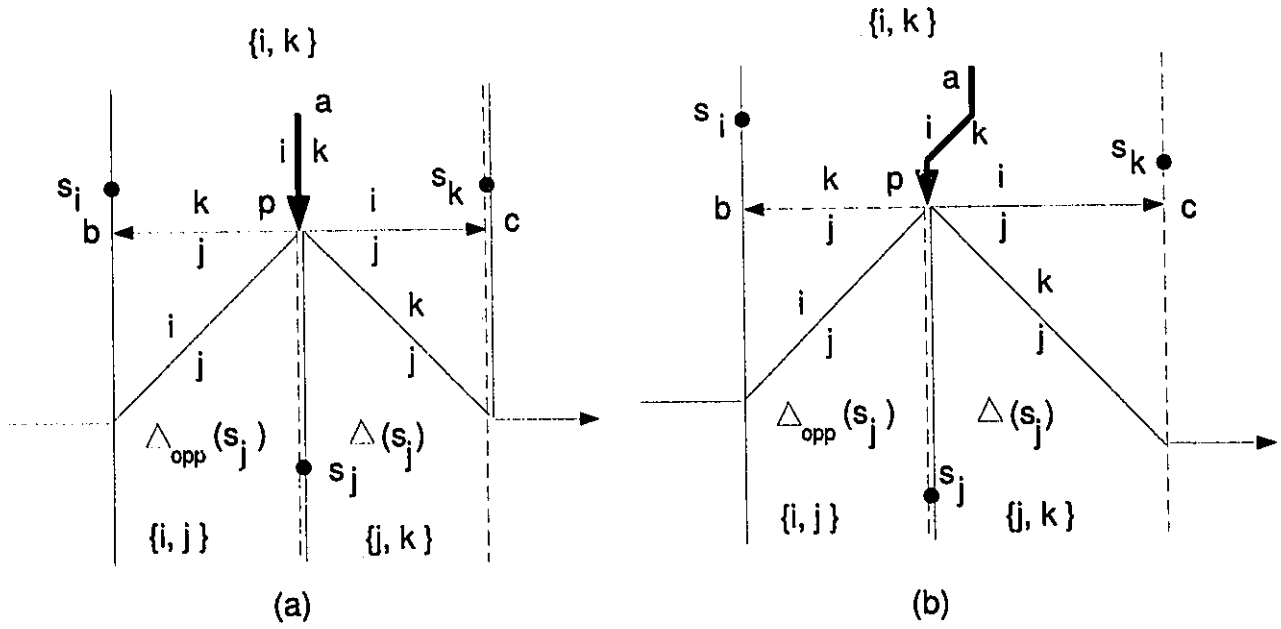
Figure 29 (b) is a special situation of *case 5* (figure 29 (a)), where  $\overline{s_i p} = \overline{s_j p} = \overline{s_k p}$ .

*Case 6:* If the two sites  $s_i$  and  $s_k$  of an area  $\{i, k\}$  have the same y-coordinate, (figure 30 (a)) the bisector is a straight line (figure 4 (h)). Let  $\overline{ap}$  be a type 2 Voronoi arc of area  $\{i, k\}$ . If the ending point  $p$  of  $\overline{ap}$  is the position where two h\_SPM arcs  $\overline{pb}$ ,  $\overline{pc}$  join (apparently, these two h\_SPM arcs are on a straight line). This is the same situation as in case 5, that three sites ,  $s_i$ ,  $s_j$  and  $s_k$  are vertices of a isosceles triangle. Check from  $D_{st}$  (DCEL), if this edge is already recorded inside, that is, check if the other two type 2 Voronoi arcs are already traced in a type 2 Voronoi arc tree. If it is inside  $D_{st}$ , delete edge  $\overline{ap}$  from  $D_{st}$  (DCEL). Get the h\_SPM arc  $\overline{pb}$  with the left (right) side field  $\Delta_{opp}(s_j)$  ( $\Delta_{opp}(s_k)$ ), get the h\_SPM arc  $\overline{pc}$  with the left (right) side field  $\Delta(s_i)$  ( $\Delta(s_j)$ ). Determine the two adjacent areas,  $\{i, j\}$  and  $\{j, k\}$ . Compute their type 2 Voronoi arcs, save one type 2 Voronoi arc in  $D_{st}$  for later tracing, and trace back along another type 2 Voronoi arc.

The same method can be applied in Figure 30 (b). The only difference is that

the two sites  $s_i$  and  $s_k$  of an area  $\{i, k\}$  have different y-coordinates, and their bisector is not a straight line.

Figure 30 Three type 2 Voronoi arcs meet together. Tracing type 2 Voronoi arc trees from edge  $\overline{ap}$



### Theorem 3.10

The Voronoi diagram with  $n$  sites in  $L_1$  metric can be constructed in  $O(n \log n)$  time and  $O(n)$  space.

*Proof:* From lemma 3.4, the construction of the Shortest-Path-Maps,  $SPM_{\leftarrow}(S)$  and  $SPM_{\rightarrow}(S)$  takes  $O(n \log n)$  time. After the left-to-right sweep and

right-to-left sweep, all the edges of SPMs are grouped into fields and stored in the Doubly-Connected-Edge-List (DCEL).

Tracing the type 1 Voronoi arcs and type 2 Voronoi arcs to form the Voronoi diagram starts from: (1) the  $h\_SPM$  arcs with the ending points at infinity, or the type-2 Voronoi arc with one ending point at infinity (these  $h\_SPM$  arcs and type 2 Voronoi arcs are saved in  $D_{st}$  (DCEL) during the two sweeps), or from (2) each newly found type 1 Voronoi arc (found at the time of tracing type 2 Voronoi arc trees and is treated as a starting edge of a type 2 Voronoi arc tree, or a terminating edge of a type 2 Voronoi arc tree), or from (3) each newly found type 2 Voronoi arc (three type 2 arcs meet together), and then tracing into the areas one after another.

Picking up the starting arc of a Voronoi arc tree from  $D_{st}$  takes  $O(1)$  time.

Fetching the SPM arcs which enclose an area from DCEL (an area is enclosed by a group of SPM arcs) takes  $O(1)$  time.

The total number of SPM arcs in the plane is  $O(n)$ .

Computing the intersections in each area between a type-2 Voronoi arc and the enclosing SPM arcs takes  $O(n_k)$  time where  $n_k$  is the number of enclosing SPM arcs. As every SPM arc is used a constant number of time in this way and  $\sum n_k = O(n)$ . Finding the intersections for all the areas takes  $O(n)$ .

The total number of type 1 Voronoi arcs and type 2 Voronoi arcs in the Voronoi

diagram is  $O(n)$ . Therefore, the total time required to trace out all the type 1 and type 2 Voronoi arcs takes  $O(n)$  time. Hence, the total amount of time required to construct the Voronoi diagrams of a set of  $n$  site in  $L_1$  metric is  $O(n \log n)$  ■

## **Chapter 4 Conclusions**

We presented an  $O(n \log n)$  time and  $O(n)$  space algorithm for the Voronoi diagram of a set of  $n$  sites in  $L_1$  metric using a *two plane sweep* method. The two sweeps produce two data structures, called the left-to-right Shortest-Path-Map ( $SPM_{\leftarrow}(S)$ ) and the right-to-left Shortest-Path-Map ( $SPM_{\rightarrow}(S)$ ). Each of the maps partitions the plane into regions. They contain enough information to determine the left closest site and right closest site of each point in the plane. Then by tailoring the two maps with chains of Voronoi edges, the Voronoi diagram is constructed.

A method for storing the SPM arcs in groups according to the fields they belong in the DCEL data structure is used to speed up the process.

A balanced binary search tree (T) is adopted for efficiently updating the status of the sweep line.

It is interesting to investigate if this technique can be applied to Voronoi diagrams in other metrics.

## APPENDIX 1 An Algorithm for Constructing the Left to Right Shortest Path Map ( $SPM_{\rightarrow}(S)$ )

**while** (queue is not empty) **do**

- dequeue the head element  $s_i$ . /\* the sweep line is positioned at event point  $s_i$  \*/

- Determine the upper boundary  $v_h$  of the initial region  $\Delta(s_i)$  on the sweep line  $l_i$  using a balanced binary search tree ( $T$ ).

**if** ( $v_h$  is at infinity) **then**

There is no horizontal bisector above site  $s_i$ .

Compute the type-2 Voronoi arc with one ending point at infinity, and save it in  $D_{s_i}$ .

**else**  $v_h$  is not at infinity

Computes the bisector  $B_h(s_i)$  that starts from  $v_h$  and ends at  $+\infty$ .

Insert  $B_h(s_i)$  into  $T$ .

**endif**

- Determine the lower boundary  $v_l$  of the initial region  $\Delta(s_i)$  on the sweep line  $l_i$  by a balanced binary search tree ( $T$ ).

**if** ( $v_l$  is at infinity) **then**

There is no horizontal bisector below site  $s_i$ .



Compute the type-2 Voronoi arc with one ending point at infinity, and  
save it in  $D_{st}$ .

**else**  $v_l$  is not at infinity

Computes the bisector  $B_l(s_i)$  that starts from  $v_l$  and ends at  $+\infty$ .

Insert  $B_l(s_i)$  into T

**endif**

- The bisectors truncated by the segment  $\overline{v_h v_l}$  are deleted from the tree (T).
- Save the segment  $\overline{v_h v_l}$  (including  $v_h$ ,  $v_l$  at infinity) into two DCEL groups according to their left side and right side field.
- Save each of the bisectors truncated by the segments  $\overline{v_h v_l}$  into the DCEL field groups according to their left side field and right side field.

**if** ( $s_i$  is not the last element in the ST) **then**

loop back

**else**

Save each of the bisectors (their ending point are at  $+\infty$  in the tree (T)  
into two DCEL groups according to their left side field and right side field.

Save them into  $D_{st}$  (DCEL). /\* starting edges for tracing the type 2  
Voronoi arc trees \*/

**endif**

**endwhile**

## APPENDIX 2 An Algorithm for Constructing the Voronoi Diagram in $L_1$ Metric

**while** (  $D_{st}$  is not empty) **do**

Step 1:

Dequeue  $e_{st}$  from  $D_{st}$  (DCEL) /\*  $e_{st}$  is an element in  $D_{st}$ , a starting edge for tracing a type 2 Voronoi arc tree \*/

**if** ( $e_{st}$  is a type 1 Voronoi arc) **then**

/\* see figure 26 regardless of whatever the ending point is at infinity \*/

The next area  $\{L, R\}$  where the next edge lies within is determined by the left side field  $F_L$  and the right side field  $F_R$  of  $e_{st}$ .

**else**  $e_{st}$  is a type 2 Voronoi arc

/\* that is the situation where three edges meet at a point (see Lemma 3.9). The left side field  $F_L$  and right side field  $F_R$ , that is, the area  $\{L, R\}$  is known \*/

**endif**

Step 2:

**if** (the bisector of the two sites of the area is a vertical line segment (i.e. the y-coordinates of the two sites of the area are the same) (figure 4 (h)), or

the bisector does not intersect the vertical line passing through the two sites  
(figure 4 (a) (b)), **then**

Get all the edges of the two field groups from  $D_{L_R}$  (DCEL) and  $D_{R_L}$   
(DCEL)

Compute the type 2 Voronoi arc in the current area.

Compute the intersection between the type 2 Voronoi arc and edges of  
the two field groups from  $D_{L_R}$  (DCEL) and  $D_{R_L}$  (DCEL)

Save the type 2 Voronoi arc in  $D_v$ .

**else** /\* the bisector of the two sites of the area intersects the vertical line  
passing through two sites (figure 4 (c) (d)) \*/

Get the edges of one field group from  $D_{L_R}$  (DCEL) or  $D_{R_L}$  (DCEL)  
which opposites the direction of tracing along the type 2 Voronoi arc.

Compute the type 2 Voronoi arc in the current area.

Compute the intersection between the type 2 Voronoi arc and edges of  
one field group which opposites the direction of tracing along the type  
2 Voronoi arc.

**endif**

**Case 1:** the type 2 Voronoi arc meets the  $h\_SPM$  arc of  $\Delta_{opp}(s_j)$ , (case 2 in  
*Algorithm* and figure 27),

Get the type 1 Voronoi arc which is part of the h\_SPM arc and the next area in which the next type 2 Voronoi arc lies inside.

**if** (type 1 Voronoi arc is in  $D_{end}$  (DCEL)) **then**

    Delete type 1 Voronoi arc from  $D_{end}$  (DCEL).

**else** save it in  $D_{st}$  and  $D_v$ .

**endif**

Trace the next type 2 Voronoi arc, go back to the beginning of STEP 2.

**endcase 1**

**Case 2:** the type 2 Voronoi arc meets the v\_SPM arc of  $\Delta_{opp}(s_j)$ . (see case 3 in *Algorithm* and figure 28), the next edge is a type 1 Voronoi arc.

**if** (the type 1 Voronoi arc is in the  $D_{st}$ ) **then**

    delete it from  $D_{st}$

**else** save it into  $D_{end}$

**endif**

Go back to the beginning of **while do**.

**endcase 2**

**Case 3:** the type 2 Voronoi arc meets at the corner of a site field, (cases 5, 6 in *algorithm* Lemma 3.9 and figures 29, 30), the corner is the intersection of three type 2 Voronoi arcs.

**if** (this type 2 Voronoi arc is in  $D_{st}$ ) **then**

delete it from  $D_{st}$  /\* the other two type 2 Voronoi arc was traced  
before \*/

go back to beginning of **while do**.

**else** save one type 2 Voronoi arc into  $D_{st}$  (and  $D_v$ ), trace the other type  
2 Voronoi arc.

**endif**

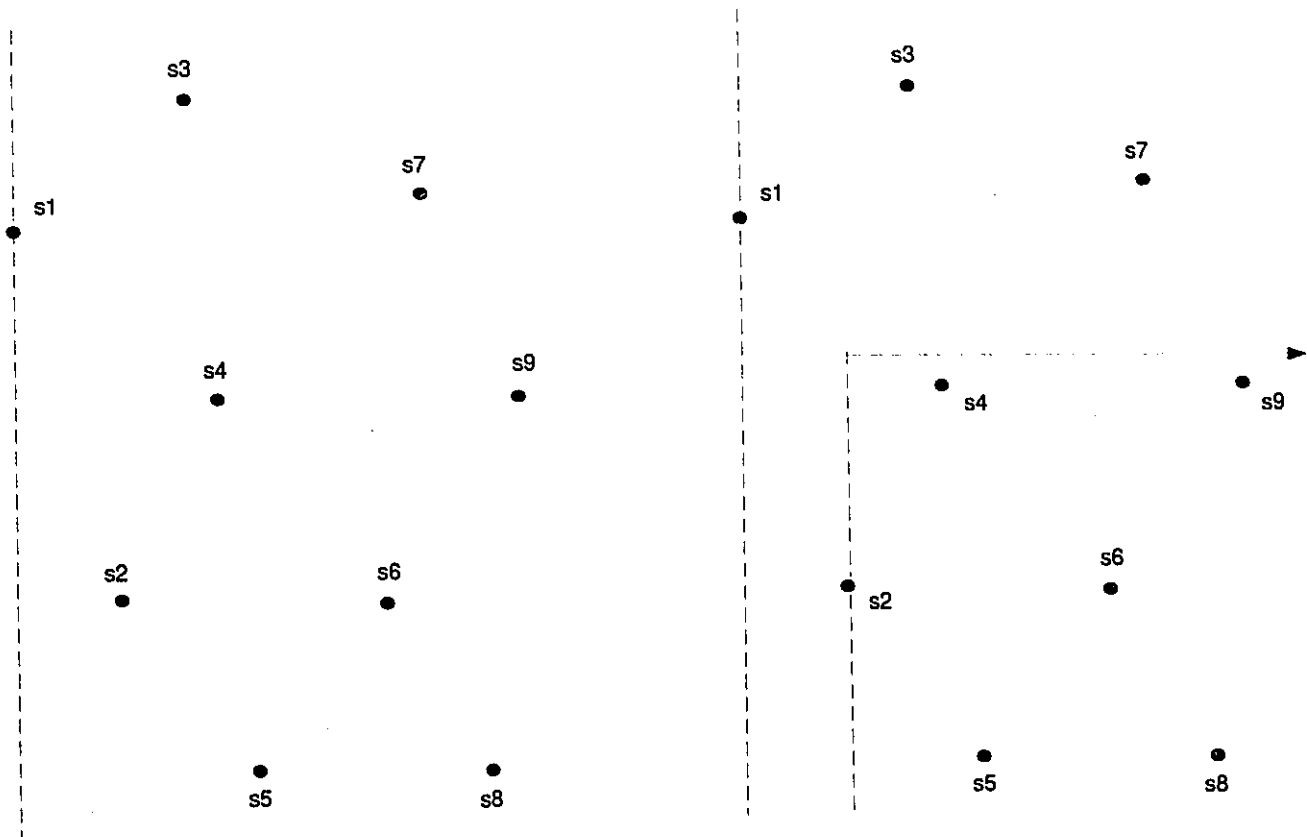
Go back to Step 2.

**endcase 3**

**endwhile**

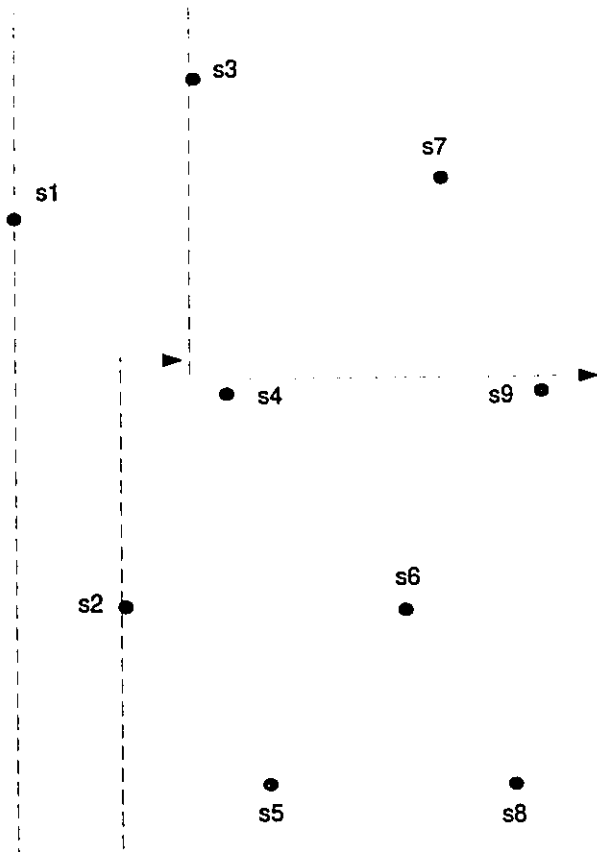
### APPENDIX 3 An Example of Constructing the Voronoi Diagram in $L_1$ Metric

The example below illustrates how the left to right sweep and the right to left sweep work, how the *areas* are formed by the two sweeps, and how the Voronoi arcs are constructed.

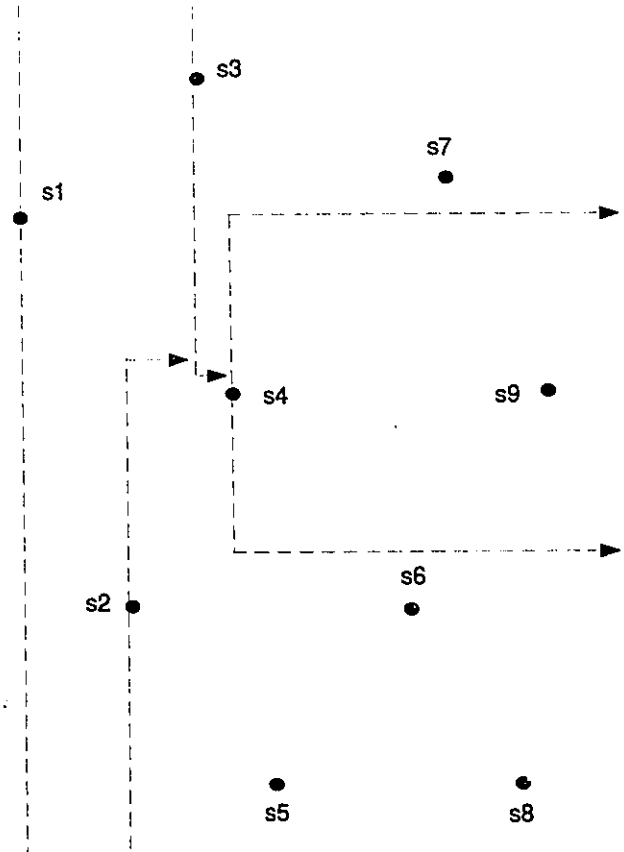


(a) Sweep line at site  $s1$

(b) Sweep line at site  $s2$

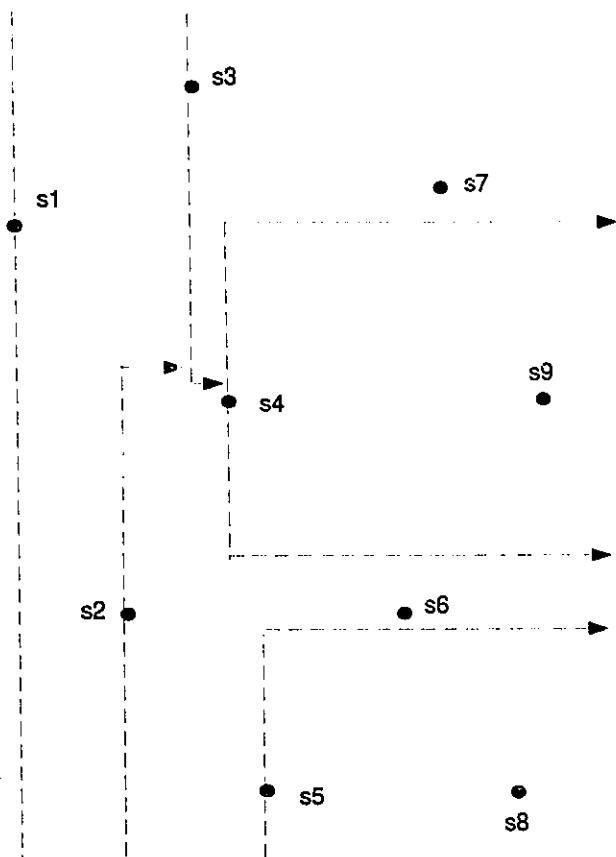


(a) Sweep line at site  $s_3$

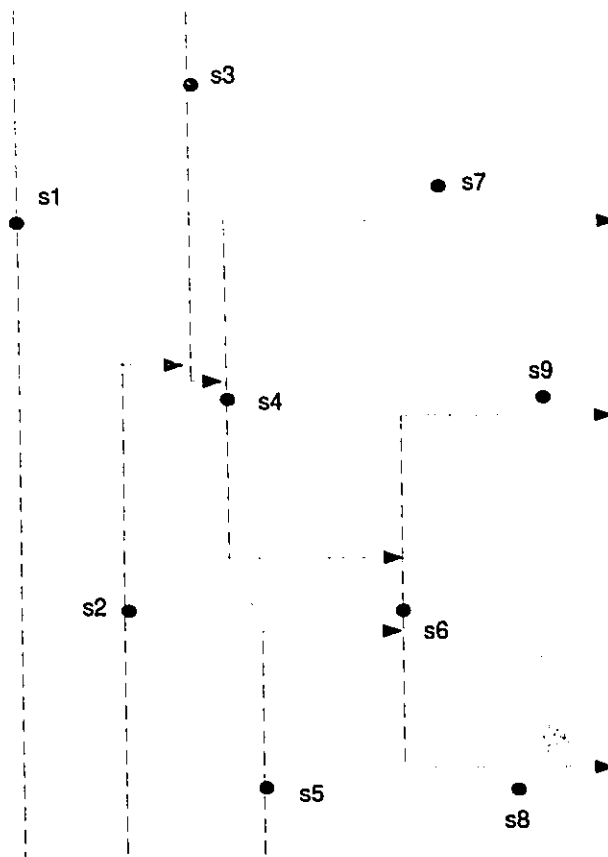


(b) Sweep line at site  $s_4$

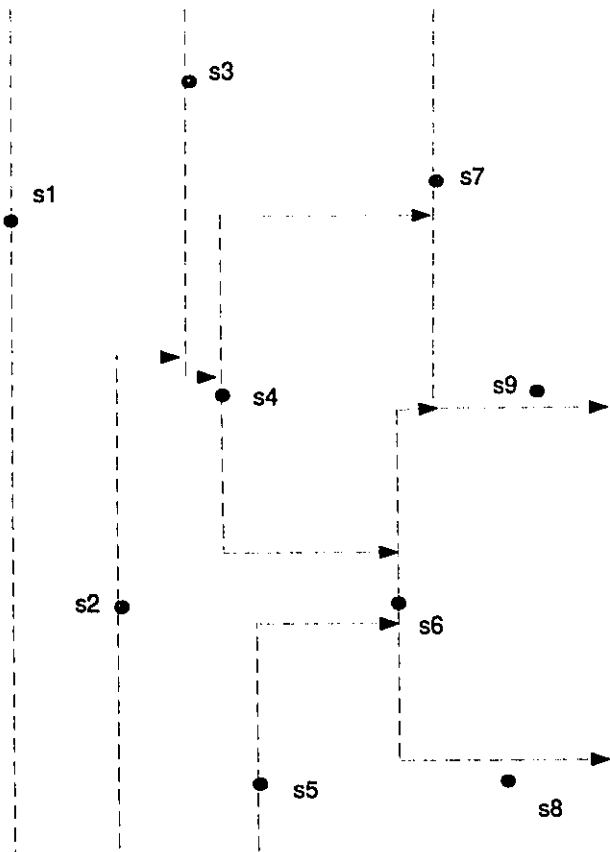




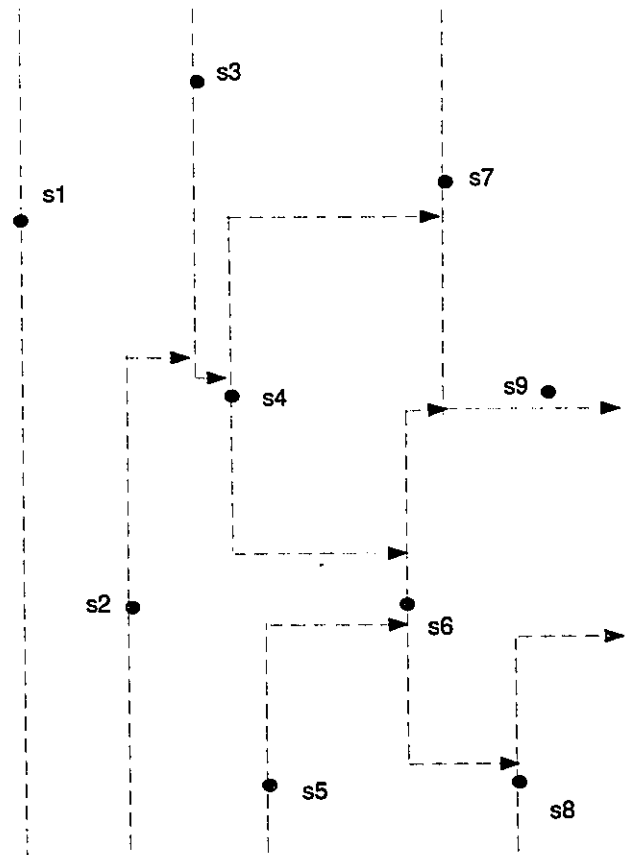
(a) Sweep line at site  $s_5$



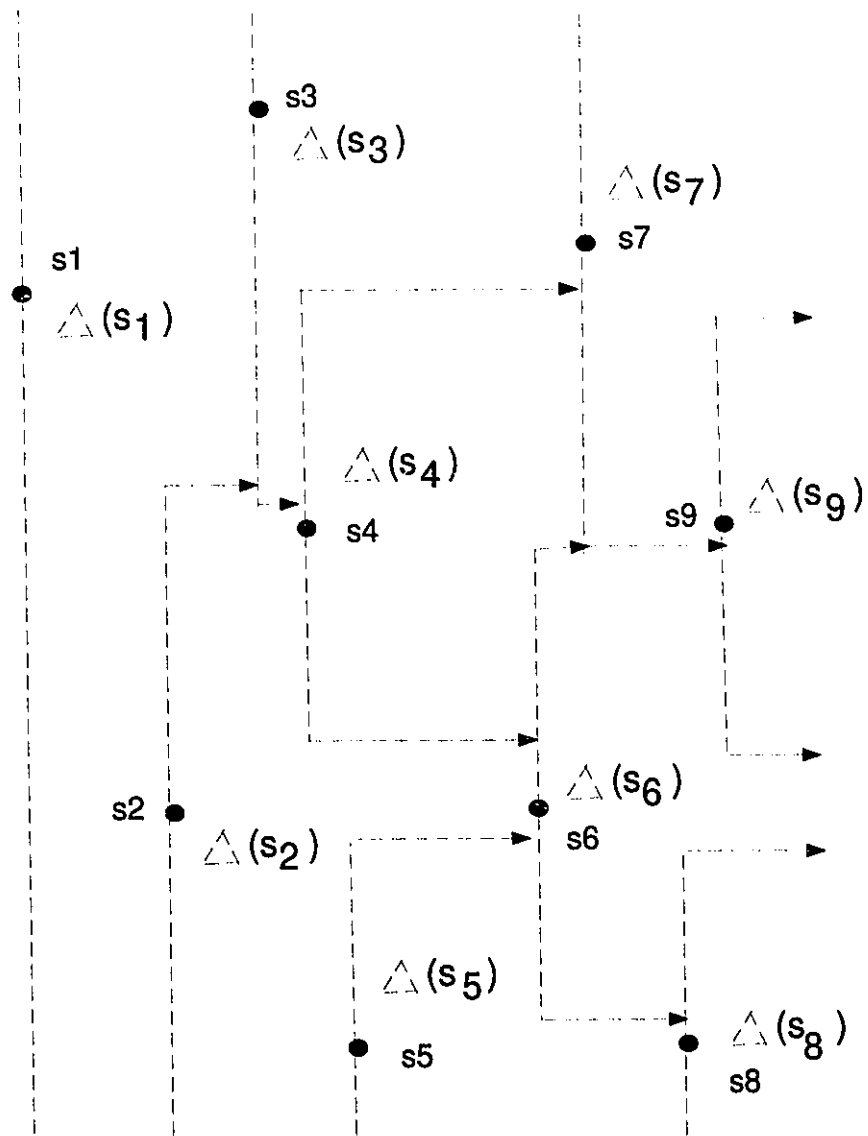
(b) Sweep line at site  $s_6$



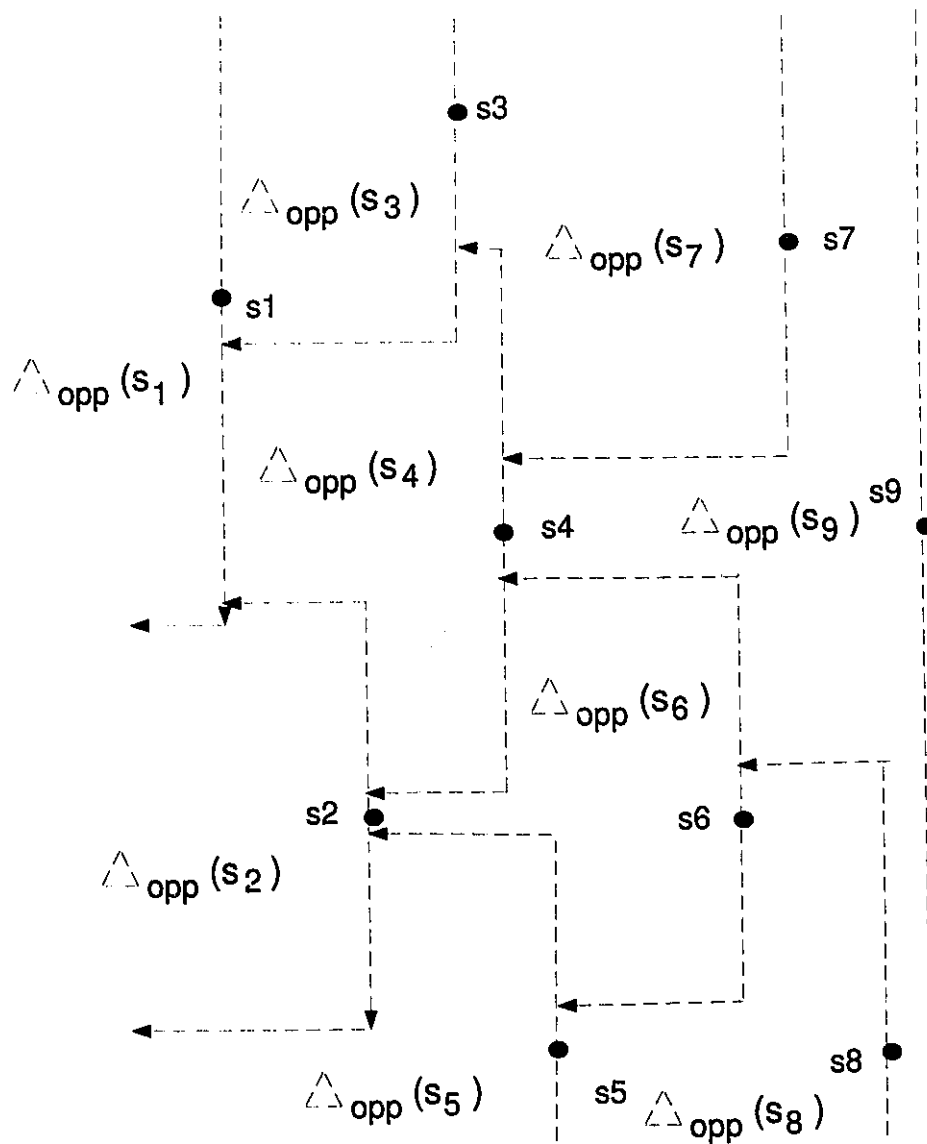
(a) Sweep line at site s7



(b) Sweep line at site s8

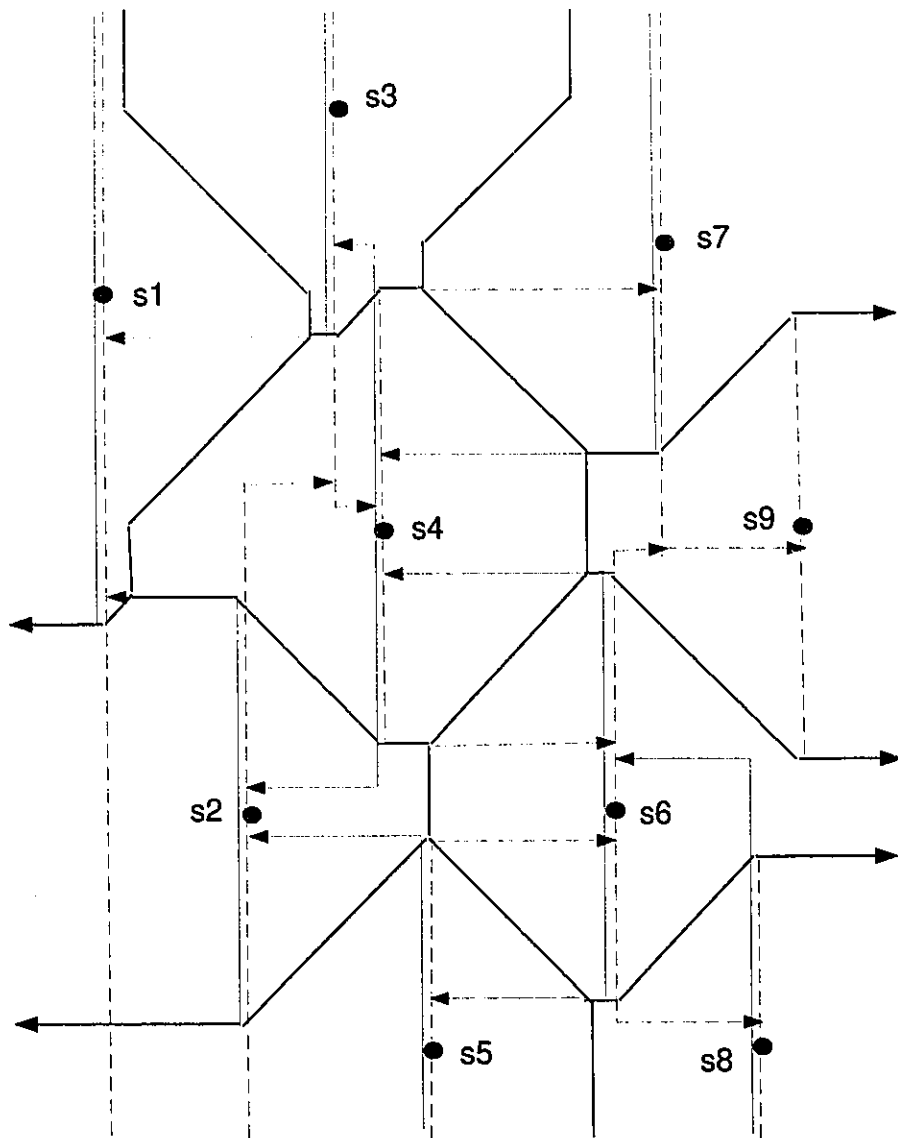


The left to right SPM  $\mapsto (S)$

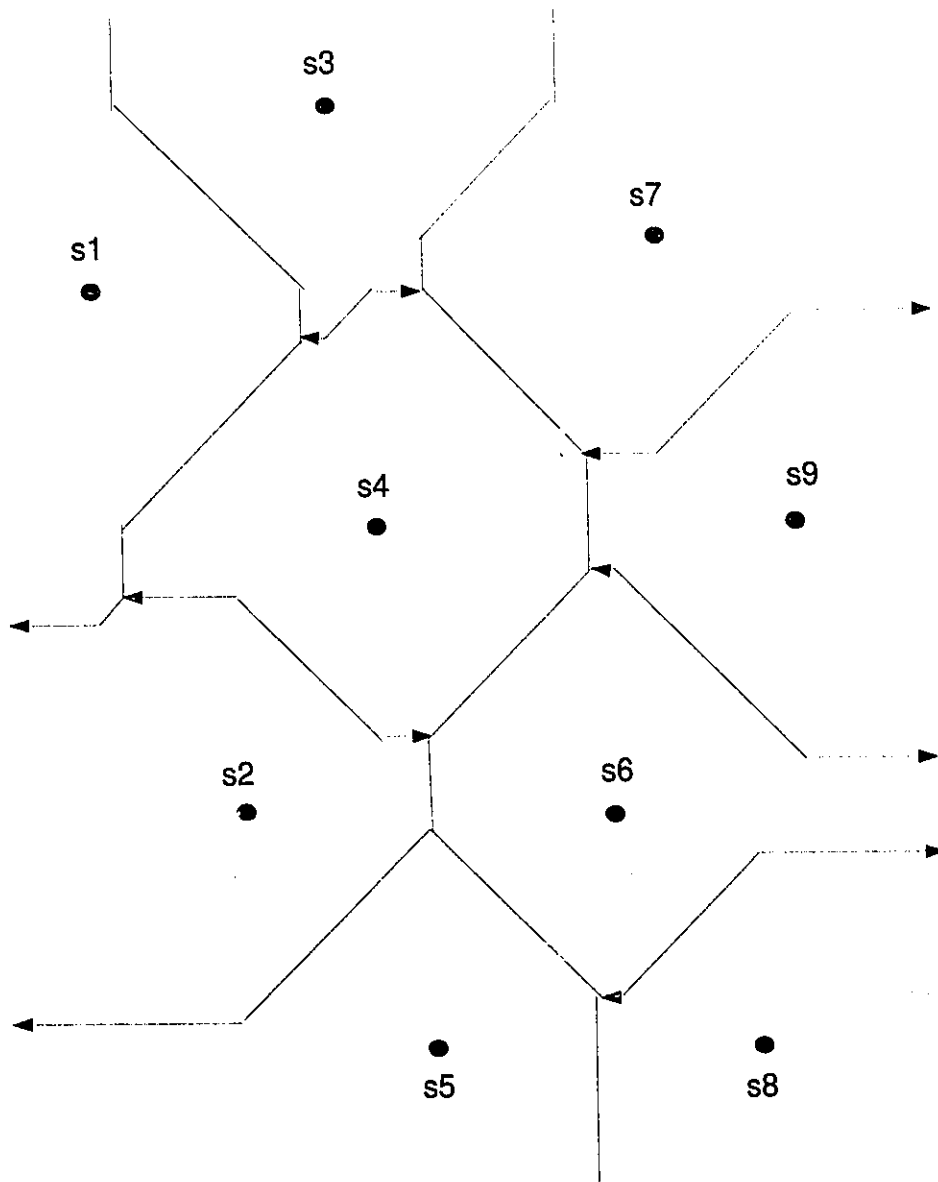


The right to left  $\text{SPM} \leftarrow (S)$





Voronoi arcs are traced



Voronoi diagram in  $L_1$  metric

## BIBLIOGRAPHY

- [1] F. Aurenhammer and H. Edelsbrunner. An optimal algorithm for constructing the weighted voronoi diagrams in the plane. *Pattern Recognition*, vol. 17, no. 2, pp. 251–257, 1984.
- [2] J.R. Bitner and C.K. Wong. Optimal and near-optimal scheduling algorithms for batched processing in linear storage. *SIAM J. on Computing* 8, pp. 479–499, 1979.
- [3] K.Q. Brown. Voronoi diagram from convex hulls. *Inform. Process Letter*, 9, pp. 223–228, 1979.
- [4] P. Chew and R.L. Drysdale III. Voronoi diagrams based on convex distance functions. *1st ACM Annual Symposium on Computational Geometry*, pp.235–244, 1985.
- [5] R.L.III Drysdale and D.T. Lee. Generalization of voronoi diagram in the plane. *SIAM J. Comput.* vol. 10, no. 1, Feb. 1981.
- [6] R.L.III Drysdale and D.T. Lee. Generalized voronoi diagram in the plane. *Proc. of the 16th Annual Allerton Conference on Communications, Control and Computing*, pp. 833–842, Oct. 1978.
- [7] H. Edelsbrunner, J. O'Rourke, and R. Seidel. Constructing arrangements of lines and hyperplanes with applications. *SIAM J. Comput.* 15, pp.341–363, 1986.
- [8] S.J. Fortune. A sweep line algorithm for voronoi diagrams. *Proc. 2nd Ann. ACM Symp. Comput. Geom.* pp.313–322., 1986.
- [9] P. Green and R. Sibson. Computing dirichlet tessellations in the plane. *Compt. J.* 21, pp.168–173.
- [10] F.K. Hwang. An  $O(n \log n)$  algorithm for rectilinear minimal spanning trees. *ACM* vol. 26, no. 2, pp.177–182, April 1979.
- [11] H. Imai, M. Iri, and K. Murota. Voronoi diagram in the laguerre geometry and its applications. *SIAM J. Comput.* vol.14, no.1, pp. 93–105, Feb. 1985.
- [12] D.G. Kirkpatrick. Efficient computation of continuous skeletons. *Proc. 20th IEEE Annu. Symp. Found. Comput. Sci.*, pp.18–27, Oct. 1979.



- [13]D.T. Lee. Farthest neighbor voronoi diagrams and applications. *Dep. Elec. Eng. Comput. Sci., Northwestern Univ., Evanston, IL. Tech. Rep. 80-11-FC-04*, 1980.
- [14]D.T. Lee. On k-nearest neighbor voronoi diagram in the plane. *IEEE Trans. on Comput.*, 35(6), pp. 478-487, June 1982.
- [15]D.T. Lee. On k-nearest neighbor voronoi diagrams in the plane. *IEEE Transaction on Computers*, 35(6), pp. 478-487, June 1982.
- [16]D.T. Lee. On finding k-nearest neighbors in the plane. *Technical report, Coordinated Sci. Lab., Univ. of Ill., Urbana, Illinois*, May 1976.
- [17]D.T. Lee. Two dimensional voronoi diagram in the  $l_p$  metric. *J. of ACM*, vol. 27, no.4, pp. 604-618, Oct. 1980.
- [18]D.T. Lee and F.P. Preparata. The all nearest neighbor problem for convex polygons. *Info. Proc. Lett.*, 7, pp. 189-192, 1978.
- [19]D.T. Lee and F.P. Preparata. Euclidean shortest paths in the presence of rectilinear barriers. *Networks*, vol.14, pp. 393-410, 1984.
- [20]D.T. Lee and C.K. Wong. Voronoi diagrams in  $l_1$  and  $l_\infty$  metrics with 2-dimensional storage applications. *SIAM J. on Comput.* vol. 9, No.1, pp.200-212, Feb. 1980.
- [21]A. Lingas. Voronoi diagrams with barriers and shortest diagonal problem. *Information Processing Letters*, 32:191-198, 1989.
- [22]D.E. Muller and F.P. Preparata. Finding the intersection of two convex polyhedra. *Theoretical Computer Science*, 7(2), pp. 217-236, Oct. 1978.
- [23]F.P. Preparata. Steps into computational geometry. *Tech. Report, Coordinated Science Lab., Univ. of Illinois, Urbana, Il.*, 1977.
- [24]R. Seidel. Constrained delaunay triangulation and voronoi diagrams with obstacles. *Rep.260*, pp.178-191, IIG-TV Graz, Austria, 1988.
- [25]M.I. Shamos. Computational geometry. *PhD thesis, Dept. of Comput. Sci., Yale Univ.*, 1978.
- [26]M.I. Shamos. Geometric complexity. *Proc. 7th ACM Annu. Symp. Theory Comput.* pp.224-233, May 1975.
- [27]M.I. Shamos and D. Hoey. Closest-point problems. *Proc. 16th IEEE Ann. Symp. Found. Comput. Sci.* pp. 208-215, 1976.
- [28]B. Shneiderman and V. Goodinan. Batched searching of sequential and tree structured files. *ACM Trans. Database Sys.* 1, pp. 268-275, 1976.

- [29]M.I. Shomas and F.P. Preparata. Computational geometry. *Spring Verlag*, 1985.
- [30]Y.H. Tsin and C. Wang. Finding constrained and weighted voronoi diagrams in the plane. *Proceedings of the Second Canadian Conference in Computational Geometry*, pp. 200–303, 1990.
- [31]Y.H. Tsin and C. Wang. Finding geodesic voronoi diagram of points in the presence of rectilinear barriers. 1990.
- [32]G. Voronoi. Nouvelles applications des paramètres continues à la théorie des formes quadratiques; premier mémoire: sur quelques propriétés des formes quadratiques positives parfaites. *J. Reine Angew. Math.* 133, pp. 97–178, 1907.
- [33]G. Voronoi. Nouvelles applications des paramètres continues à la théorie des formes quadratiques; deuxième mémoire; recherches sur les paralléloèdres primitifs. *J. Reine Angew. Math.* 134, pp.198–287, 1908.
- [34]C. Wang and L. Schubert. An optimal algorithm for constructing the delaunay triangulation of a set of line segments. *3rd ACM Annual Symposium on Computational Geometry*, pp.223–232, 1987.

## **VITA AUCTORIS**

**Jianan Wang** graduated from the Department of Electrical Engineering and Computer Science at Shanghai Jiao Tong University with a Bachelor of Science in 1982. He then worked at The Ninth Design and Research Institute China State Shipbuilding Corporation, and later at Shanghai China Cooperation for Foreign Economic and Technological Corporation (Australia Branch).

He is currently a candidate for the Master's degree in Computer Science at the University of Windsor and expected to graduate in Sept. 1994.